



## **Testing Revisions to RRTMG Cloud Radiative Transfer in HWRF**

Michael J. Iacono and John M. Henderson  
Atmospheric and Environmental Research  
131 Hartwell Avenue, Lexington, Massachusetts 02421-3126  
(E-mail: [miacono@aer.com](mailto:miacono@aer.com))

### **Final Project Report**

Developmental Testbed Center (DTC) Visitor Program 2016

March 2017

## 1. Overview

The main objective of this project for the Developmental Testbed Center Visitor Program was to implement and test revisions to HWRF (*Bernardet et al.*, 2015) related to the treatment of cloud radiative transfer in the RRTMG radiation code developed at AER (*Iacono et al.*, 2008). NOAA adopted RRTMG for operational use in HWRF\_v3.7 during the 2015 hurricane season. The specific cloud radiation change investigated relates to the radiative coupling of clouds and the treatment of vertical cloud overlap, which can strongly impact radiative fluxes and heating rates. The default cloud overlap assumption in RRTMG, known as maximum-random, has been compared to an alternate method known as exponential-random to establish the impact of revising this important cloud-radiative process on the prediction of tropical cyclones in HWRF. Forecasts of multiple tropical cyclones has shown a significant response in atmospheric heating rates due to the cloud overlap change that alters the atmospheric state to a sufficient degree that tropical cyclone track and intensity are affected in some cases.

## 2. Background

### *Cloud Overlap*

The representation of the sub-grid scale properties of clouds in dynamical models remains a significant source of uncertainty in weather forecasts and climate projections. This uncertainty relates to the horizontal inhomogeneity of cloud microphysical properties and the vertical correlation or overlap of clouds and their impacts on cloud radiative processes. Understanding each of these effects is critical to predictions of the atmosphere (*Wu and Liang*, 2005). Biases associated with these processes have been shown to compensate to some degree (*Nam et al.*, 2012; *Shonk et al.*, 2010b), which reinforces the need both to study them independently and to improve them in combination.

Of importance to this effort is the application within RRTMG of the Monte-Carlo Independent Column Approximation (McICA; *Barker et al.*, 2007; *Pincus et al.*, 2003), which is a statistical technique for representing the sub-grid variability of clouds within the radiative transfer calculations. At present, McICA is used to represent the cloud fraction and vertical correlation of clouds. McICA could also be used to represent the sub-grid variations of other cloud properties, though this capability was not utilized in this project. Cloud overlap assumptions in RRTMG include random (no correlation between disassociated, separated cloud layers), maximum (fully overlapping in the vertical within adjacent, multiple cloud layers), and a blend of these two called maximum-random (maximum overlap in adjacent cloud layers and random overlap among separated groups of cloud layers) first described by *Geleyn and Hollingsworth* (1979).

For this project, RRTMG\_LW and SW were modified to incorporate an additional cloud overlap method in order to test its impact on tropical cyclone forecasts. Although maximum-random is the most commonly used overlap assumption in dynamical models, a more recent variation of this approach called exponential-random (*Hogan and Illingworth*, 2000; *Shonk, et al.*, 2010a) is also coming into use. This method presumes the vertical correlation within a group of adjacent cloud layers transitions inverse exponentially from maximum to random with increasing distance. The exponential transition,  $\alpha$ , from maximum to random within continuous

cloud layers is defined as a function of distance through the cloud,  $\Delta z$ , and a decorrelation length,  $Z_{0\alpha}$ ,

$$\alpha = e^{-(\Delta z/Z_{0\alpha})} . \quad [1]$$

Smaller vertical distances through the cloud and larger decorrelation lengths ( $\alpha \rightarrow 1$ ) infer a greater tendency toward maximum overlap while larger distances through the cloud and smaller decorrelation lengths ( $\alpha \rightarrow 0$ ) infer a tendency toward random overlap. Typical values of  $Z_{0\alpha}$  vary from about 1.5 km at higher latitude to 3.5 km near the equator. Based on the work of *Pincus et al.* (2005) a constant decorrelation length of 2 km was applied in this work. Evaluating other constant values of  $Z_{0\alpha}$  and implementing an alternate method in which  $Z_{0\alpha}$  varies spatially will be the subject of future research.

Cloud overlap treatments in dynamical models have gradually evolved as surface radar and satellite observations have revealed better statistics about the vertical structure of clouds. For example, it is known that maximum overlap occurs preferentially in deep clouds in areas of strong ascent and convective instability (*Shonk et al.*, 2010b; *Geer et al.*, 2009), though this assumption is less effective in vertically oriented clouds in regions with strong wind shear (*Pincus et al.*, 2005). This conclusion suggests that a cloud overlap method that varies with meteorological conditions would be more effective than a global approach. Surface radar measurements of clouds support this theory and the application of regional variations in cloud overlap method that depend on atmospheric conditions (*Naud et al.*, 2008) and season (*Mace and Benson-Troth*, 2002). Radar observations also validate the assumption of exponential decay from maximum to random overlap with increasing vertical distance through multiple cloud layers (as defined in the exponential-random treatment) rather than the simple assumption of maximum overlap in deep clouds (as presumed in the maximum-random method). The effectiveness of any cloud overlap assumption is also dependent on the spatial resolution of the dynamical model.

The exponential-random (ER) method is in effect a compromise between the more extreme random and maximum-random (MR) assumptions. This compromise is illustrated in Figure 1, which shows differences in longwave upward, downward and net flux profiles (top panels) and cooling rate profiles (bottom panels) in the standard tropical atmosphere as calculated by RRTMG\_LW using ER (with a decorrelation length of 1 km) and MR cloud overlap for three cloud cases. Cloud case 1 is all liquid with cloud fraction of 0.5 in each layer with cloud water paths varying from 5 to 10  $\text{gm}^{-2}$  and particle effective radii from 5 to 10 microns from cloud top to bottom. Cloud case 2 has a cloud fraction of 0.5 in each layer and transitions from ice above about 600 hPa to liquid below with cloud water paths varying from 1 to 10  $\text{gm}^{-2}$  and particle effective radii from 10 to 25 microns. Cloud case 3 has two blocks of clouds, one all ice above and one all liquid below, with similar physical properties as cloud case 2. In Figure 1, flux differences as high as 25  $\text{Wm}^{-2}$  occur within the convective cloud and cooling rate differences peak near 1.0-1.5  $\text{Kd}^{-1}$  in all cases. A similar comparison of shortwave flux and heating rate profiles between the ER and MR overlap methods (not shown) results in somewhat smaller differences than in the longwave. However, the profile of differences in the shortwave is very different, which suggests that modifying the overlap treatment in HWRF will result in each spectral region having distinct impacts on the synoptic scale.

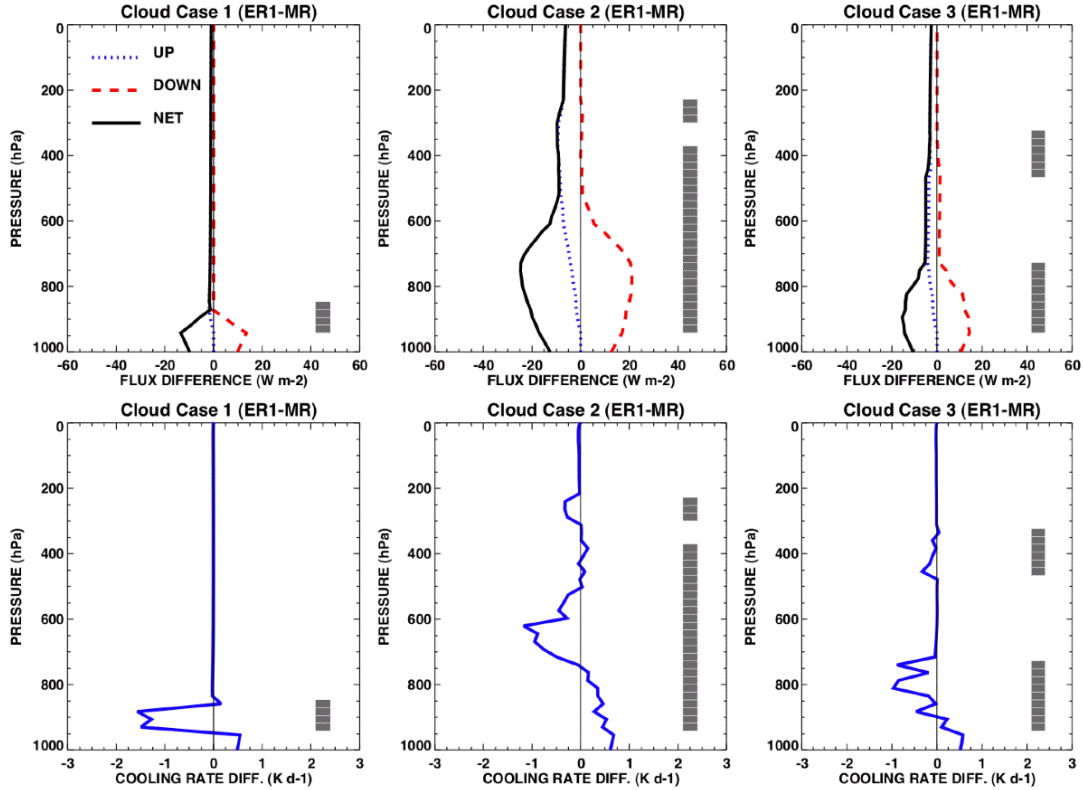


**Figure 1.** Longwave upward, downward and net flux (top) and cooling rate (bottom) profile differences calculated by RRTMG\_LW/McICA between runs using exponential-random (ER1) cloud overlap with a decorrelation length of 1 km and maximum-random (MR) cloud overlap for three cloud configurations (gray boxes).

### *HWRF Configuration*

During the course of this project, the DTC upgraded HWRF from the “H215” version to the “H216” version. Although initial setup work for the project was completed with the H215 model, the H216 model was eventually used in the tropical cyclone forecasts completed for this project that are discussed in this document. A relevant component of the H216 model is the new cloud fraction parameterization developed by Dr. Greg Thompson, which was designed to provide a more realistic distribution of fractional cloudiness in HWRF. The option is activated using the ICLOUD=3 WRF name-list setting. This option is especially relevant to the forecasts performed for this project, since the cloud overlap assumption used in the radiative transfer is strongly dependent on the sub-grid cloud fraction defined by the host model. All HWRF runs used the RRTMG longwave and shortwave radiation options and the three standard H216 nested grids with grid spacing of 18, 6, and 2 km where the outer grid is initialized with GFS model data. Each of the three tropical cyclones examined were forecast using multiple 126-hour forecast cycles that were initialized at 6-hour intervals. In each case, the initial forecast cycle was a “cold start” from GFS initial conditions and subsequent forecast cycles were a “warm start” in that the atmospheric state was derived from the previous forecast cycle (with the exception of the default vortex relocation at the start of each run). This arrangement ensured that the effects of the cloud overlap modifications were carried from one forecast cycle to the next through any atmospheric state changes.

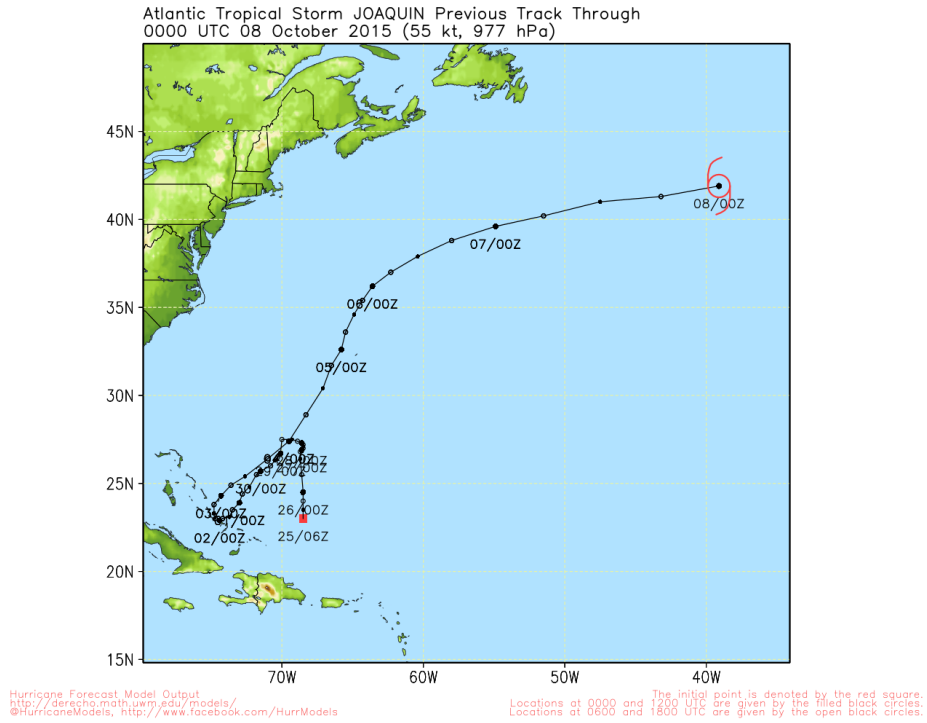


**Figure 2.** Best track path of Hurricane Joaquin through the northwest Atlantic from 25 September to 8 October 2015.

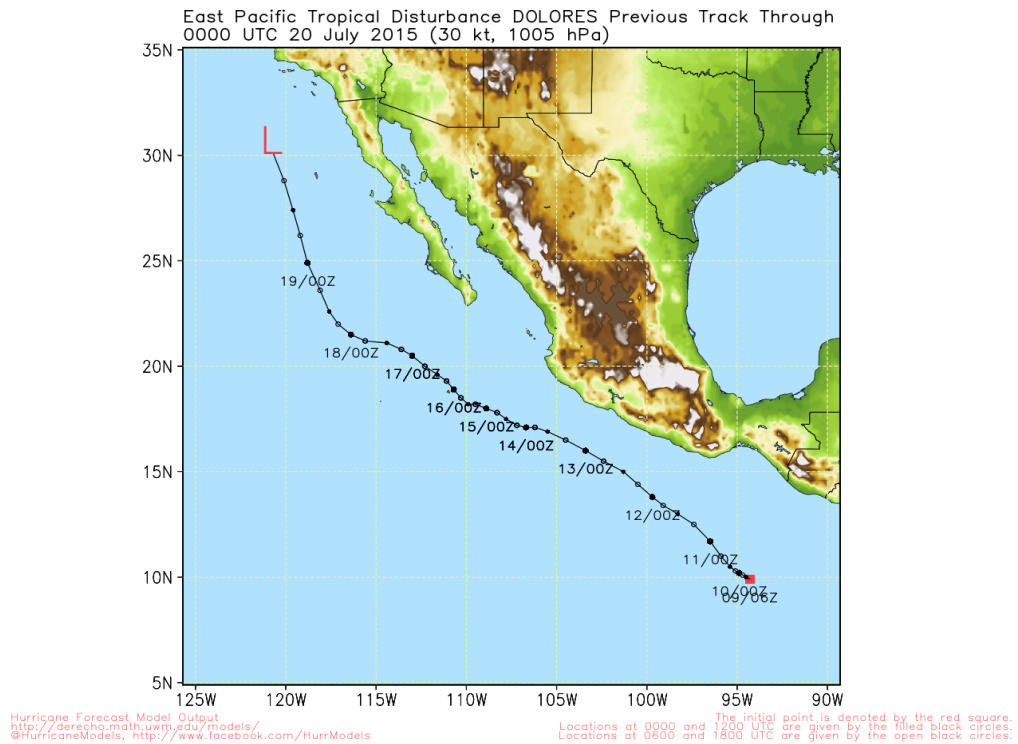


**Figure 3.** Best track path of Hurricane Dolores through the eastern Pacific basin from 11-19 July 2015.

### Tropical Cyclone Cases

This project assessed the impacts of the cloud overlap change for three tropical cyclone cases (Joaquin, Dolores, and Gonzalo). Hurricane Joaquin was an Atlantic (ATL) basin TC that was active from 25 September to 8 October 2015. This storm reached Category 4 intensity and followed a highly unusual track through the northwestern Atlantic, shown in Figure 2, which remained a forecasting challenge for many of the operational, hurricane forecast models through much of the storm's lifetime. This storm's interaction with the synoptic features that directed its track was chosen for this project due to its potential sensitivity to any atmospheric state changes caused by the cloud overlap modification. Hurricane Dolores was an East Pacific (EPAC) basin TC that was active from 11-19 July 2015 and reached Category 4 intensity. Dolores followed a relatively straight path toward the northwest, as shown in Figure 3, that remained over the ocean and paralleled the west coast of Central America. This case was relatively well forecast operationally in terms of the storm track (though intensity predictions were somewhat too weak. It was selected to illustrate whether the cloud overlap changes adversely affected the prediction of a TC track that was generally well forecast. Finally, Hurricane Gonzalo was an Atlantic basin TC that was active from 11-20 October 2014 and also reached Category 4 intensity. The track of Gonzalo was more typical of a western Atlantic hurricane in that it moved northwestward near the northern Caribbean before turning northeastward into the north Atlantic. The track of this storm was also forecast relatively well by the operational hurricane models.

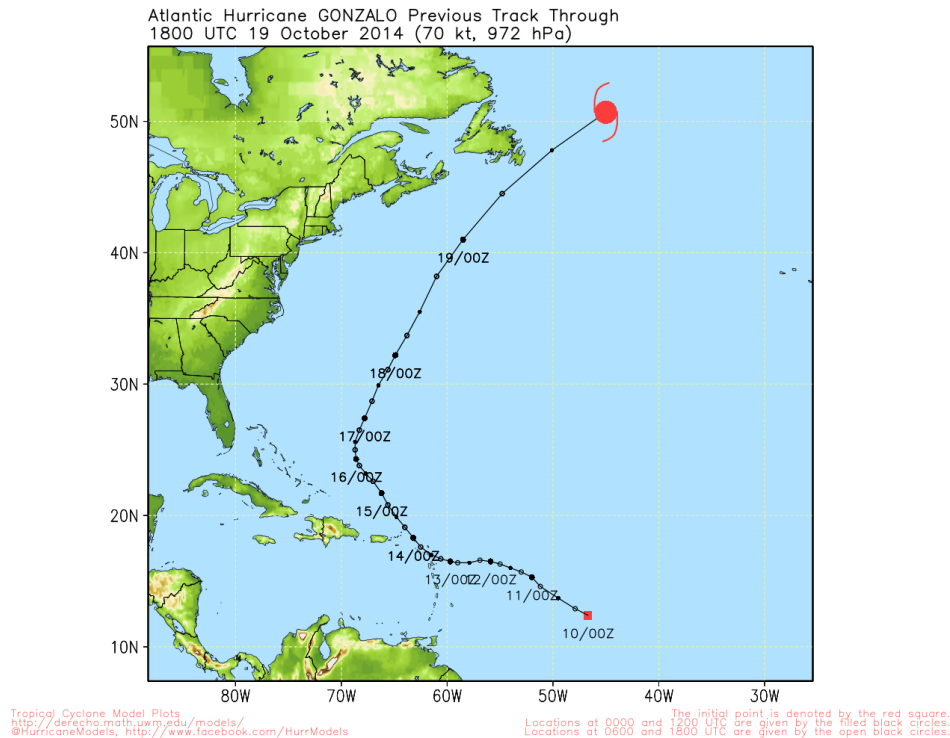


**Figure 4.** Best track path of Hurricane Gonzalo through the northwest Atlantic basin from 11-20 October 2014.

### 3. Results and Discussion

#### *Atmospheric Impacts: Radiative Heating Rates*

Our initial objective in diagnosing the impact of replacing the MR cloud overlap assumption with the ER method on TC evolution is to demonstrate that the change sufficiently alters the longwave and shortwave radiative heating rates to affect the atmospheric environment. Along with surface fluxes, the radiative heating rates are the primary means by which the radiative transfer influences the atmosphere. So, the cloud overlap modification is unlikely to affect TC evolution unless it first alters the vertical heating rate profiles. In addition, the radiative heating rate profile contains information related to all of the atmospheric parameters that were input into the radiation code, such as temperature, gas concentrations, cloud properties, etc. and the details of the heating rates provide information about the radiative influence of these parameters on the atmospheric state and TC structure.

Few opportunities are available to validate modeled radiative heating rate (HR) profiles with observations, though a derived heating rate product is available that is based on measurements from the NASA CloudSat instrument. These products consist of vertical slices along the satellite path such as the longwave heating rate cross-section through Hurricane Julia taken at 04 UTC on 15 September 2010 shown in Figure 5. A database of all such intercepts through tropical cyclones has been made available (*Tourville et al., 2015*). Application of these data to validating HWRF modeled heating rates near TCs will be addressed in future research.

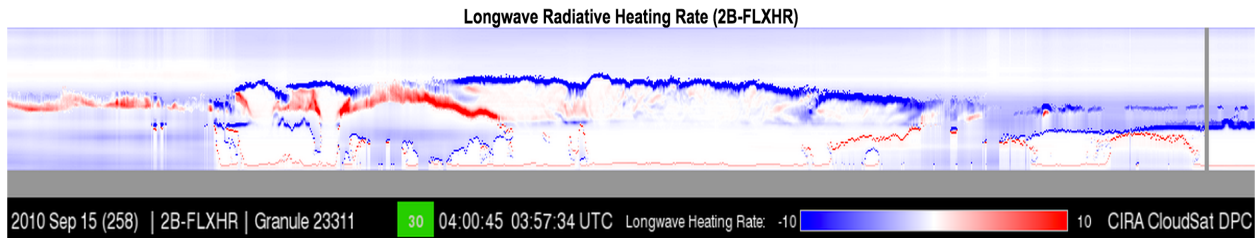


**Figure 5.** Longwave heating rate vertical cross section as derived from NASA CloudSat measurements for an intercept along the satellite path through Hurricane Julia at 04 UTC on 15 September 2010. Red denotes longwave heating and blue denotes longwave cooling.

Changes in modeled radiative heating rates due to exchanging the cloud overlap method were established by looking at “snapshots” in time of both horizontal maps and vertical slices through Hurricane Joaquin during its mature phase. Figure 6 shows the longwave radiative heating rate as predicted by HWRF (on the inner 2-km grid) using the RRTMG radiation with MR cloud overlap (left panel) and ER cloud overlap (right panel) near 900 hPa for the region around Hurricane Joaquin at 12 UTC on 2 October 2015, four days and six hours into a forecast cycle initialized at 06 UTC on 28 September 2015. Red colors in Figure 6 indicate longwave radiative heating and blue colors indicated longwave cooling. Very distinct HR patterns (and differences in the patterns) are apparent in each panel with the positive (heating) values occurring in the vicinity of highly absorbing and emitting dense cloud cover, while negative (cooling) values indicate clear or less cloudy regions. Both the extensive spiral bands of clouds and the cooler central eye typically seen in mature hurricanes are clearly visible. The large HR differences at this time and pressure level to the west through south of the storm center strongly suggest that the atmospheric state has been altered between the forecasts.

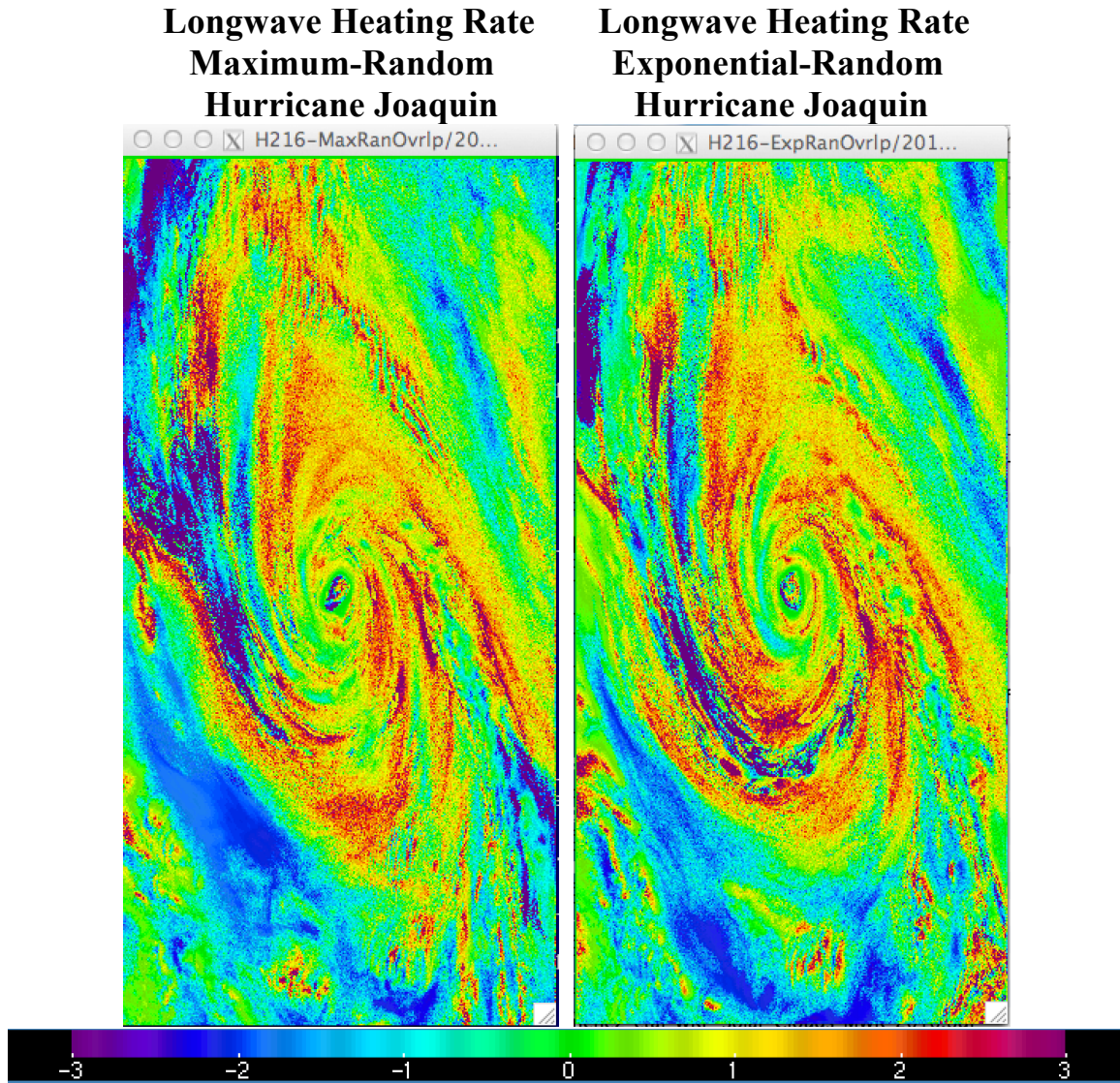


**Figure 6.** Longwave heating rate at roughly 900 hPa in the vicinity of Hurricane Joaquin as predicted by HWRP using MR cloud overlap (left) and ER cloud overlap (right) at 12 UTC on 2 October 2015 from a forecast cycle initialized at 06 UTC on 28 September 2015. Red colors denote longwave heating and blue colors denote longwave cooling. The geographic range of the plotted area is 25.6N to 34.5N and 80.0W to 69.7W. Units are  $\text{Kd}^{-1}$ .

In the manner of the CloudSat vertical cross-section heating rate product, the modeled HR differences can be diagnosed by examining vertical slices through the modeled tropical cyclones. First, it is insightful to illustrate how the background longwave heating rate profile appears in a typical tropical atmosphere. For this purpose, a height by longitude slice of longwave HR in the tropics (near 20 N) is shown in Figure 7. The vertical scale in Figure 7 is linear and the image is dominated by the troposphere. This cross-section is also dominated by clear sky as indicated by the negative heating (cooling) rates throughout much of the troposphere. Scattered small cumulus and clusters of cumulus clouds that generate longwave heating and also increase the HR below the clouds interrupt the clear sky background. The slightly positive heating values across the upper part of the image represent the tropopause, and these values revert to cooling rates upward into the stratosphere.

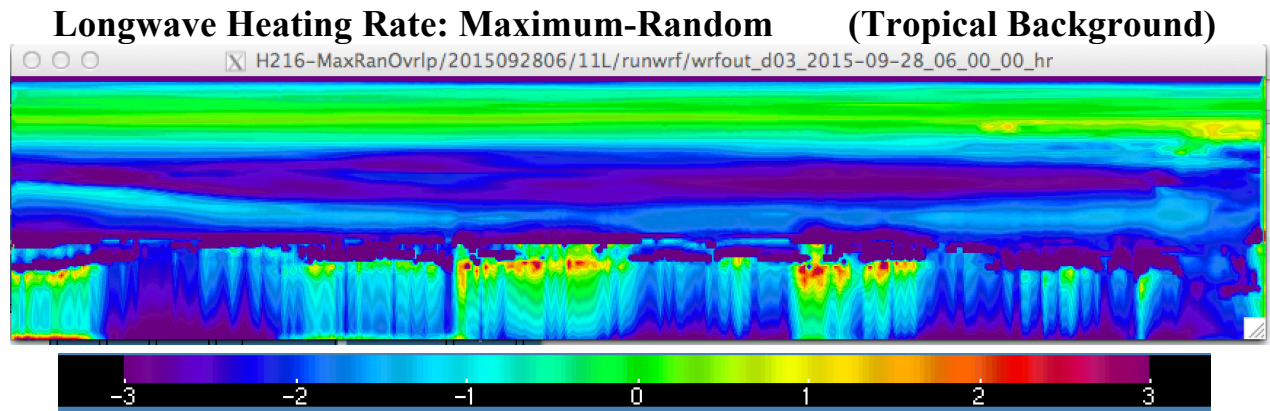


**Figure 7.** Longwave heating rate vertical cross section over the longitude range 80.0W to 69.7W at latitude 25.6N at 12 UTC on 2 October 2015 as predicted by HWRF. Red colors denote longwave heating and blue colors denote longwave cooling. The vertical scale is linear in pressure and is dominated by the troposphere. Positive values across the top of the image represent the lower stratosphere. Units are  $\text{Kd}^{-1}$ .

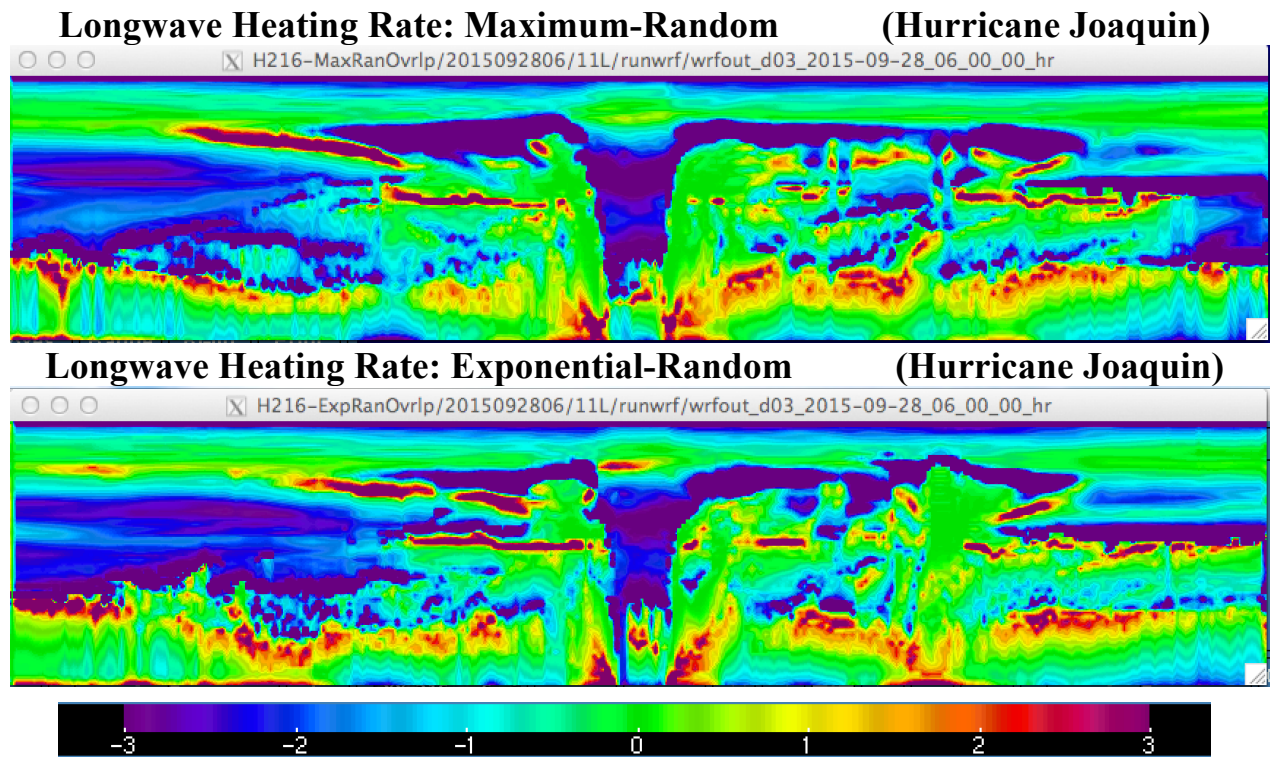


**Figure 8.** Height-by-longitude cross-sections of longwave heating rate as predicted by HWRF using MR cloud overlap (top) and ER overlap (bottom) over the inner grid longitude range 80.0W to 69.7W at latitude 30.1N at 12 UTC on 2 October 2015 directly through the center of Hurricane Joaquin. Units are  $\text{Kd}^{-1}$ .

In contrast to the typical tropical pattern of longwave heating rate in Figure 7, the comparable height-by-longitude slice directly through the center of mature Hurricane Joaquin as predicted by HWRF using MR overlap (top panel) and ER overlap (bottom panel) at 12 UTC on 2 October 2015 is shown in Figure 8. Numerous features related to tropical cyclone structure are

apparent in the heating rate cross-sections. The central eye of the storm in the middle of each panel is largely clear (longwave cooling) from the middle to upper troposphere, while clouds are present (longwave heating) in the lower part of the eye. The eye wall around the storm center is indicated by the slightly positive values surrounding much the eye that are much more strongly positive closer to the surface. The highest heating rates in the eye wall near the surface also show a distinct outward slant with height that may reflect the configuration of the strongest convection in the eye wall. Low-level convection is apparent across much of the width of the storm, while strong heating at higher levels occurs in association with the freezing level (just above the mid-troposphere) and with portions of the higher dense overcast clouds. Differences between the MR and ER cloud overlap methods are noticeable in many areas of the plots, which strongly suggests that the physics change has sufficiently altered the atmospheric state in each forecast to create considerable variations in the longwave heating rate profiles.

It is informative to compare the HR plots in Figure 8 with the cloud fractions generated by each forecast at the same place and time. Height-by-longitude plots of layer cloud fraction are shown in Figure 9 for the same vertical slice through Hurricane Joaquin shown in Figure 8 for both the MR and ER overlap forecasts. Shown as fractions from 0 to 1, the layer cloud fractions in Figure 9 illustrate the extent of fractional cloudiness that is present throughout the TC in the lower troposphere (with the notable exceptions of the eye wall and scattered overcast patches) where the cloud overlap change can potentially act to influence the atmosphere. Above the freezing level, ice clouds are generally overcast in these predictions throughout the horizontal extent of the hurricane.

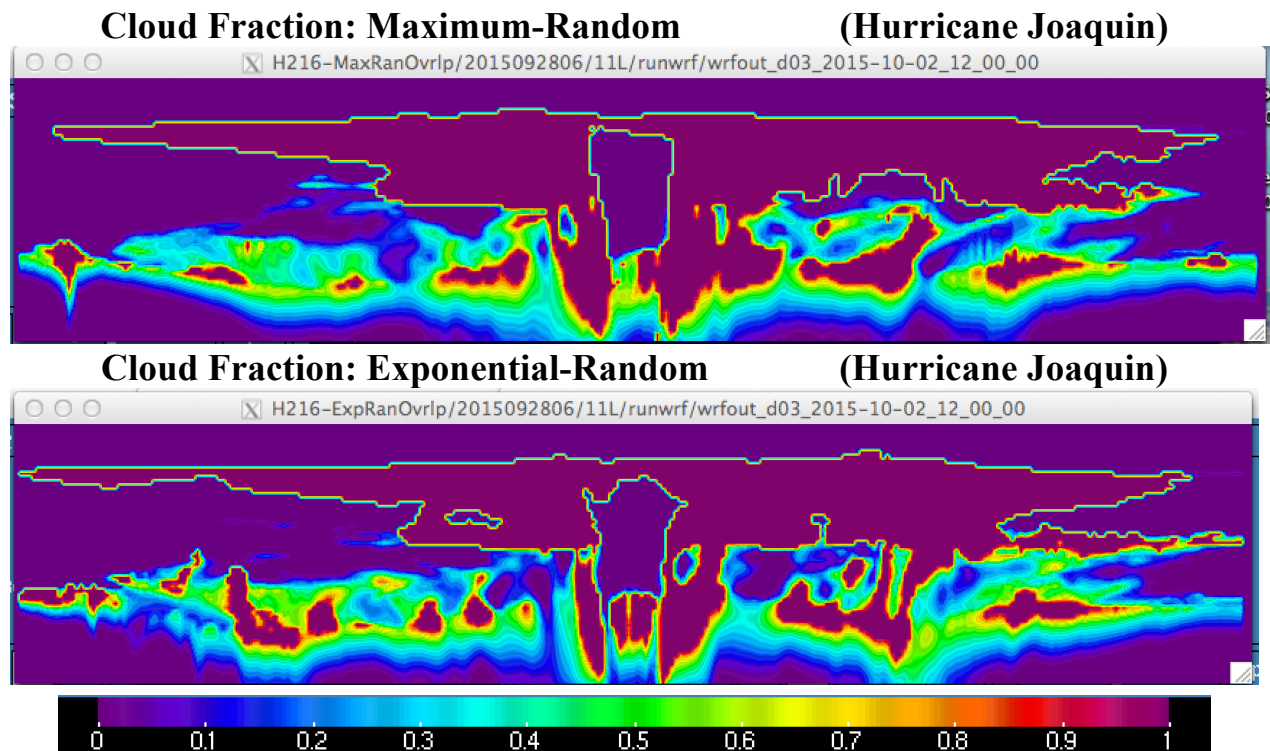


**Figure 9.** Height-by-longitude cross-sections of cloud fraction as predicted by HWRF using MR cloud overlap (top) and ER overlap (bottom) over the inner grid longitude range 80.0W to 69.7W at latitude 30.1N at 12 UTC on 2 October 2015 directly through the center of Hurricane Joaquin. Units are in fraction.

As a final example of longwave heating rate differences caused by the cloud overlap change, Figure 10 shows the height-by-longitude cross-sections from west to east through the northern eye wall of Hurricane Joaquin at the same time and about 20 km north of the plots shown in Figure 8. Here, the central eye wall feature is clearly seen to become wider with height in each forecast, with the dense absorbing and emitting clouds of the eye wall apparent near the surface while the vertical slice intersects clear sky in the upper troposphere. Although the basic pattern of features is similar between the two panels in Figure 10, there are considerable differences in the details. These include the extent of the heating within the clouds in the outflow near the top of the storm to the west of the center, the degree of strong radiative heating near the surface to the west of the center, and the vertical protrusions of convection in the ER overlap forecast to the west of the center (higher heating rate at higher vertical levels than seen in the MR overlap forecast). In addition, the horizontal extent of the eye wall appears somewhat larger in the MR forecast than with the ER overlap, as indicated by the higher heating rates that extend over a wider area around the center near the surface. Heating rate comparisons of this type offer significant potential for illustrating and diagnosing the processes related to the development and evolution of tropical cyclones.

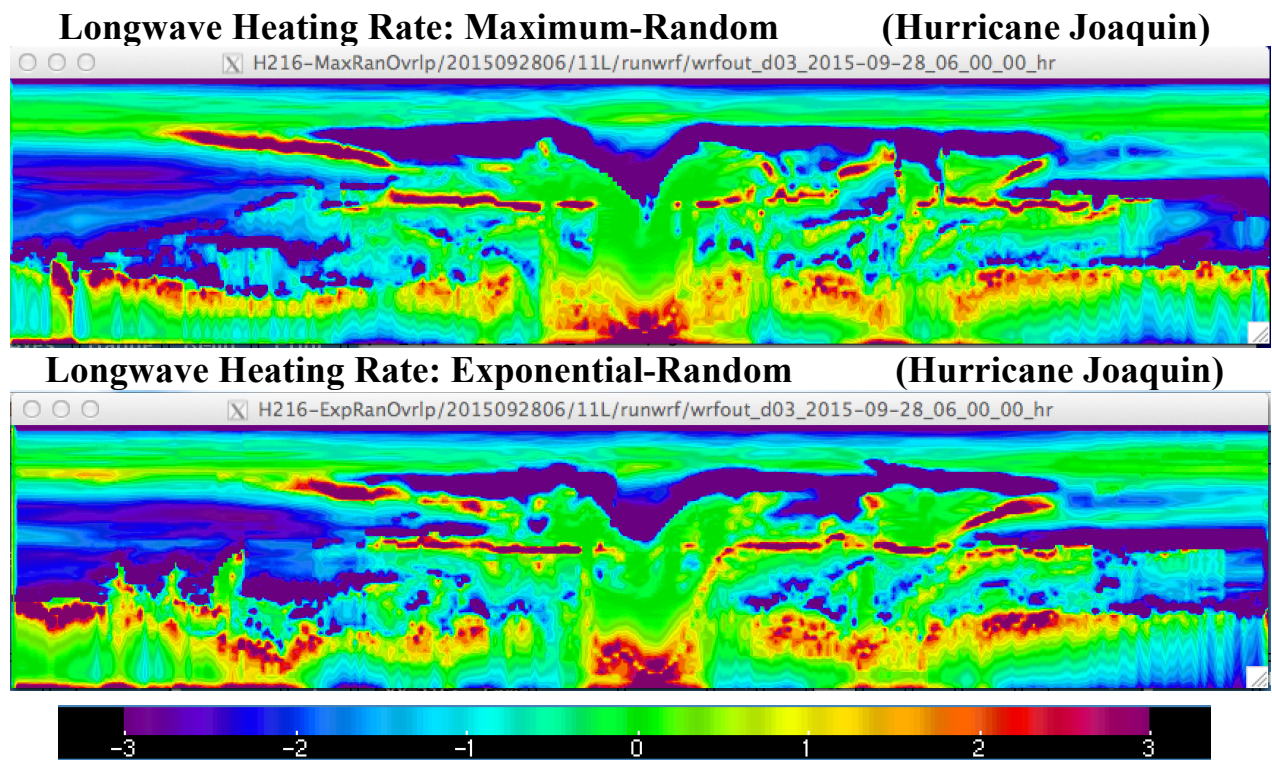


**Figure 10.** Height by longitude cross-sections of longwave heating rate as predicted by HWRF using MR cloud overlap (top) and ER overlap (bottom) over the inner grid longitude range 80.0W to 69.7W at latitude 30.5N at 12 UTC on 2 October 2015 directly through the northern eye wall of Hurricane Joaquin. Units are  $\text{Kd}^{-1}$ .

**Shortwave Heating Rate  
Maximum-Random  
Hurricane Joaquin**

**Shortwave Heating Rate  
Exponential-Random  
Hurricane Joaquin**

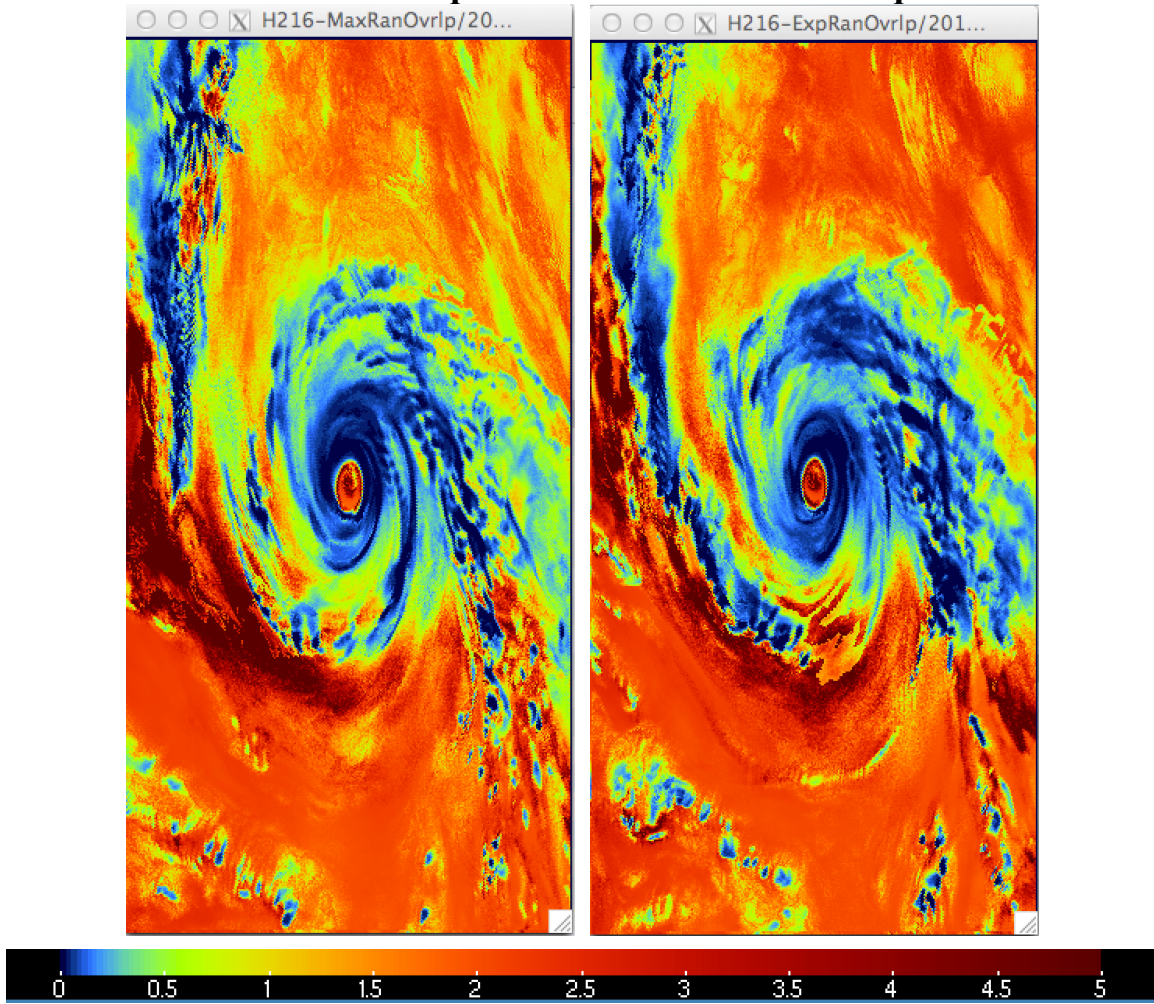


**Figure 11.** Shortwave heating rate at roughly 900 hPa in the vicinity of Hurricane Joaquin as predicted by HWRf using MR cloud overlap (left) and ER cloud overlap (right) at 18 UTC on 2 October 2015 from a forecast cycle initialized at 06 UTC on 28 September 2015. Red colors denote strong shortwave heating and blue colors denote little to no shortwave heating. The geographic range of the plotted area is 26.5N to 35.4N and 79.8W to 69.3W. At this time the storm center was located at 31.1N and 74.5W. Units are  $\text{Kd}^{-1}$ .

Heating rate differences are also seen in the shortwave part of the spectrum as indicated by the horizontal maps of shortwave heating rate in the vicinity of Hurricane Joaquin as predicted by HWRf for each cloud overlap method from the same forecast cycle but six hours later (18 UTC on 2 October 2015) than the comparable longwave plots in Figure 6. Dense cloud cover strongly reduces the shortwave heating rate around the storm center and in the cloudy spiral bands, with large differences apparent to the north, east, and southwest of the eye. Differences in the highest values of shortwave heating (fewest clouds) are noted to the west to south of the eye.

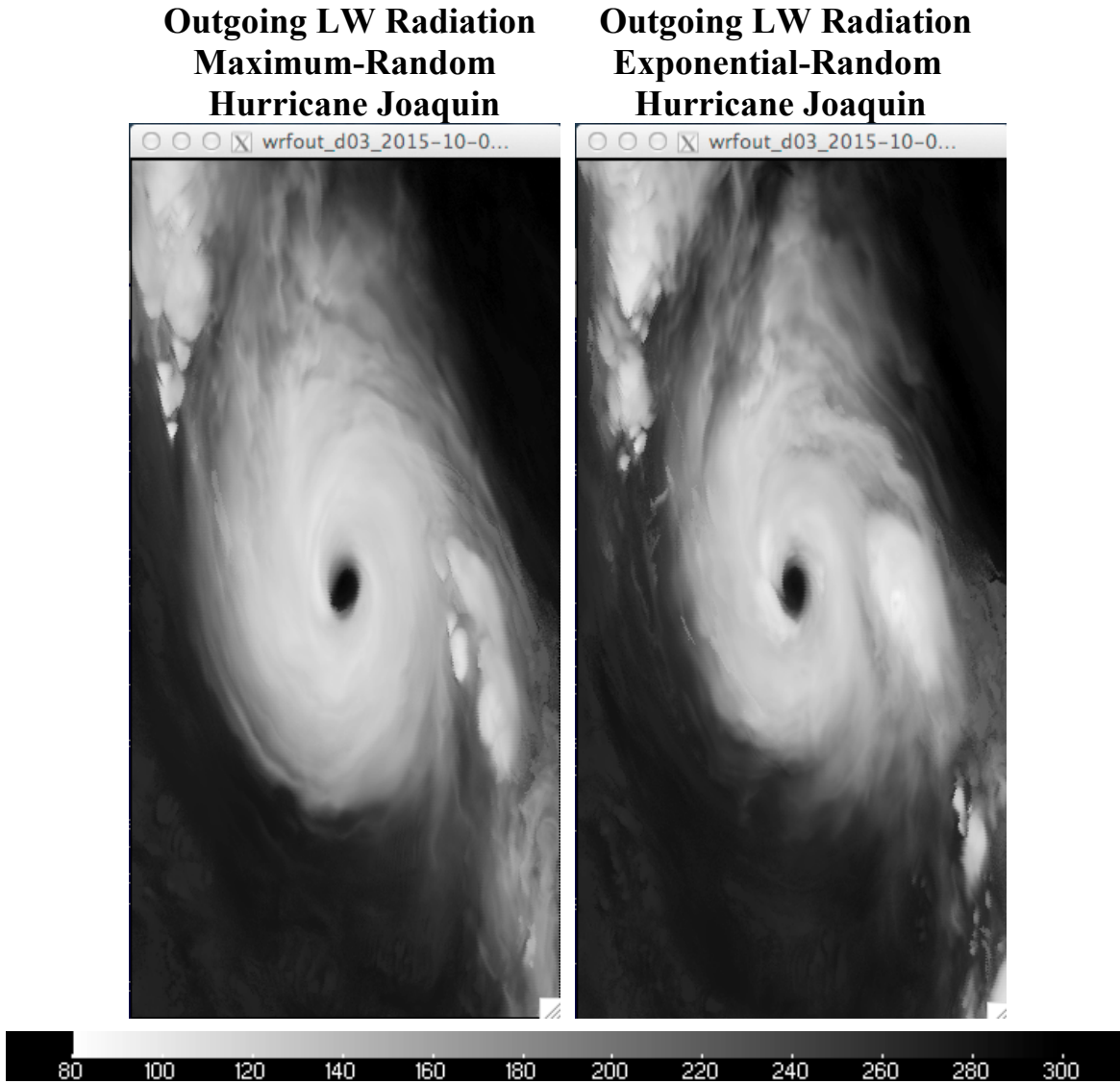


**Figure 12.** Outgoing longwave radiation in the vicinity of Hurricane Joaquin as predicted by HWRP using MR cloud overlap (left) and ER cloud overlap (right) at 12 UTC on 2 October 2015 from a forecast cycle initialized at 06 UTC on 28 September 2015. Light shades denote lower OLR and cold, high clouds while dark shades denote high OLR and clear sky or warm, low clouds. The geographic range of the plotted area is 25.6N to 34.5N and 80.0W to 69.7W. Units are  $\text{Wm}^{-2}$ .

#### *Atmospheric Impacts: Radiative Fluxes*

The extent to which the cloud overlap change impacts TC evolution can also be demonstrated by examining the top-of-the-atmosphere and surface radiative fluxes. Figure 12 shows the outgoing longwave radiation as predicted by HWRP (on the 2-km inner grid) with each cloud overlap method for the same time as the longwave heating rate plots in Figure 6. It should be pointed out again that the time plotted in Figure 12 is four days and six hours into the forecast cycle that was initialized at 06 UTC on 28 September 2015, and each forecast has had ample time to respond to the cloud overlap change and produce atmospheric state changes. In terms of the storm outflow as indicated by the horizontal extent of the coldest, high clouds (low OLR), the forecast of Hurricane Joaquin with MR overlap appears to show a larger storm than

the ER overlap forecast at this time, though the storm center itself is well-formed in both cases. An area of enhanced convection to the east of the eye appears somewhat stronger (lower OLR) in the ER case relative to the MR case, where the same feature appears somewhat weaker and further to the south. Downward shortwave surface fluxes for the same scene six hours later at 18 UTC on 2 October 2015 are shown in Figure 13. From this perspective, the ER case has generated more cloud (or more optically thick cloud) and much lower shortwave flux (blue colors) in an outer band from the north to the southeast of the eye and also within a spiral band to the southwest of the storm center. Areas of higher shortwave surface fluxes are apparent in the ER forecast to the south and west of the TC, between cloud bands and well removed from the storm center. These differences are another indication that the cloud overlap change impacts the surrounding environment, which can play a critical role in determining TC track and intensity.

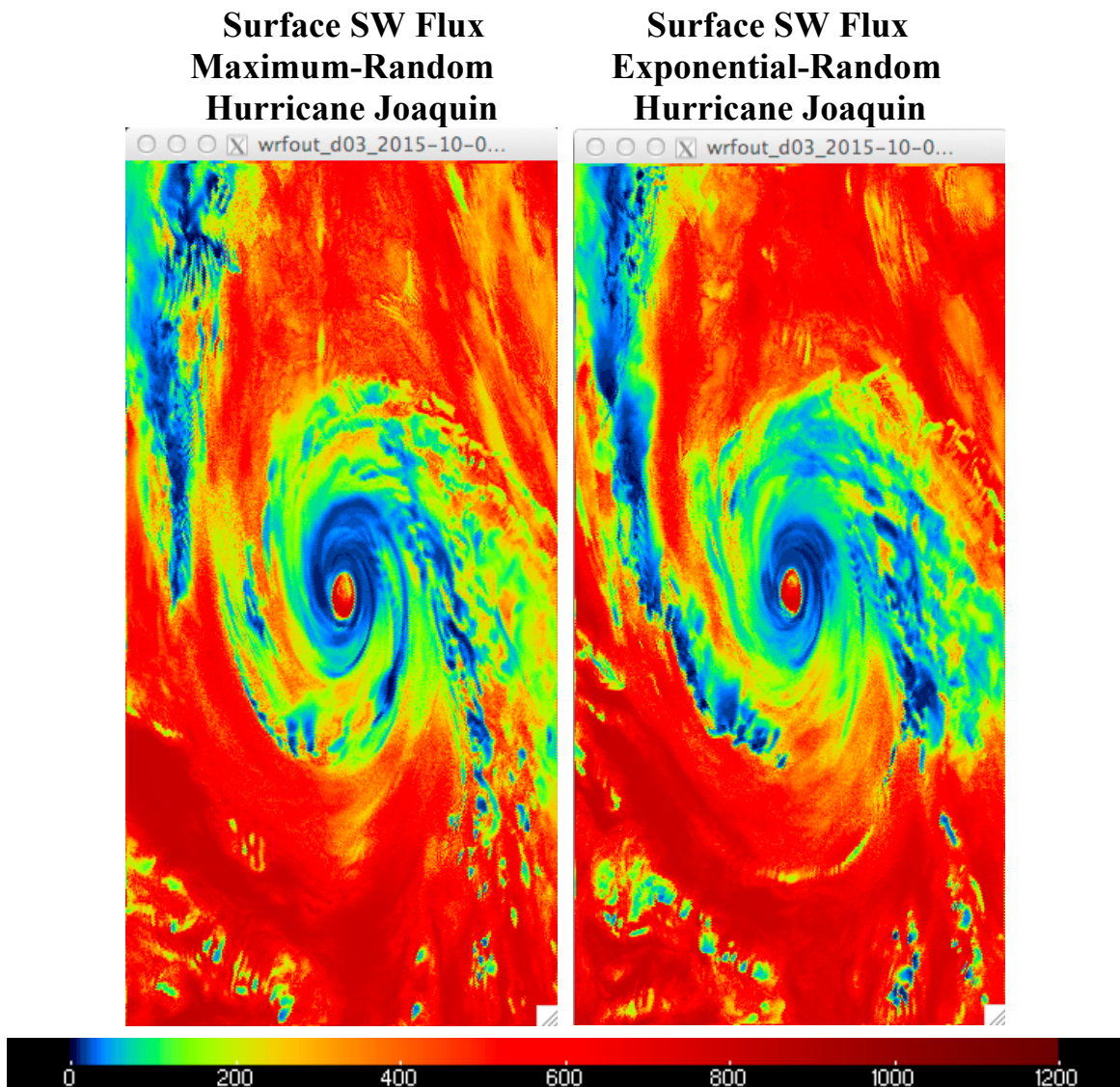


**Figure 13.** Surface downward shortwave radiation in the vicinity of Hurricane Joaquin as predicted by HWRF using MR cloud overlap (left) and ER cloud overlap (right) at 18 UTC on 2 October 2015 from a forecast cycle initialized at 06 UTC on 28 September 2015. Red colors denote higher surface flux and relatively cloud-free areas, while blue colors denote less shortwave flux reaching the surface due to opaque clouds. The geographic range of the plotted area is 25.6N to 34.5N and 80.0W to 69.7W. Units are  $\text{Wm}^{-2}$ .

*Atmospheric Impacts: Temperature, Water Vapor, and Wind Speed*

The prior section illustrated the direct influence of changing the cloud overlap method on HWRF modeled radiative fluxes and heating rates near Hurricane Joaquin, and this section will show the cumulative impact of these radiative changes on atmospheric temperature, water vapor and wind fields for this case. The left panel of Figure 14 shows the 850 hPa temperature averaged over three days from 12 UTC 30 September 2015 to 12 UTC 3 October 2015 from a HWRF forecast using MR overlap of Hurricane Joaquin from a forecast cycle initialized at 12 UTC 28 September 2015. The right panel in Figure 14 shows the corresponding three-day mean 850 hPa temperature difference for the same time period between a pair of HWRF forecasts using each overlap method (ER – MR). During this time, the predicted TC was over the northwest Atlantic between Florida and Bermuda. For this forecast cycle, the ER overlap method produces warmer 850 hPa temperatures to the northwest of the warm core of Hurricane Joaquin and in smaller areas well to the northeast and south of the storm center. Cooler temperatures are produced by the ER overlap method closer to the TC to the east through south of the center.

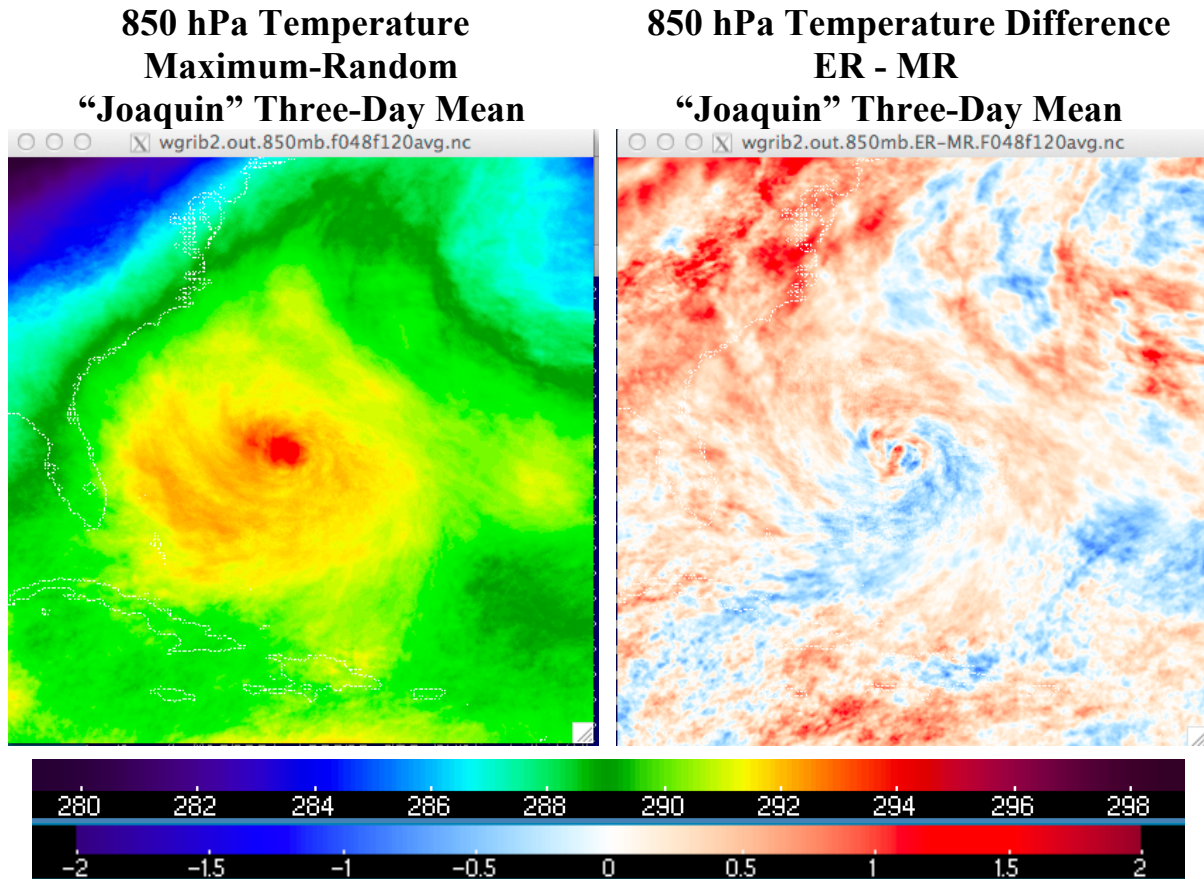


**Figure 14.** Three-day mean 850 hPa temperature in the vicinity of Hurricane Joaquin as predicted by HWRF using MR cloud overlap (left) and the three-day mean 850 hPa temperature difference for ER-MR cloud overlap (right) averaged over the period from 12 UTC 30 September 2015 to 12 UTC 3 October 2015 from a forecast cycle initialized at 12 UTC 28 September 2015. Plotted data are from the storm-following 6-km nested grid. Red colors in the right panel signify warmer temperatures in the forecast with ER cloud overlap. The geographic range of the plotted area moved over the three-day period, but it is roughly 16N to 41N and 84W to 59W. Units are K.

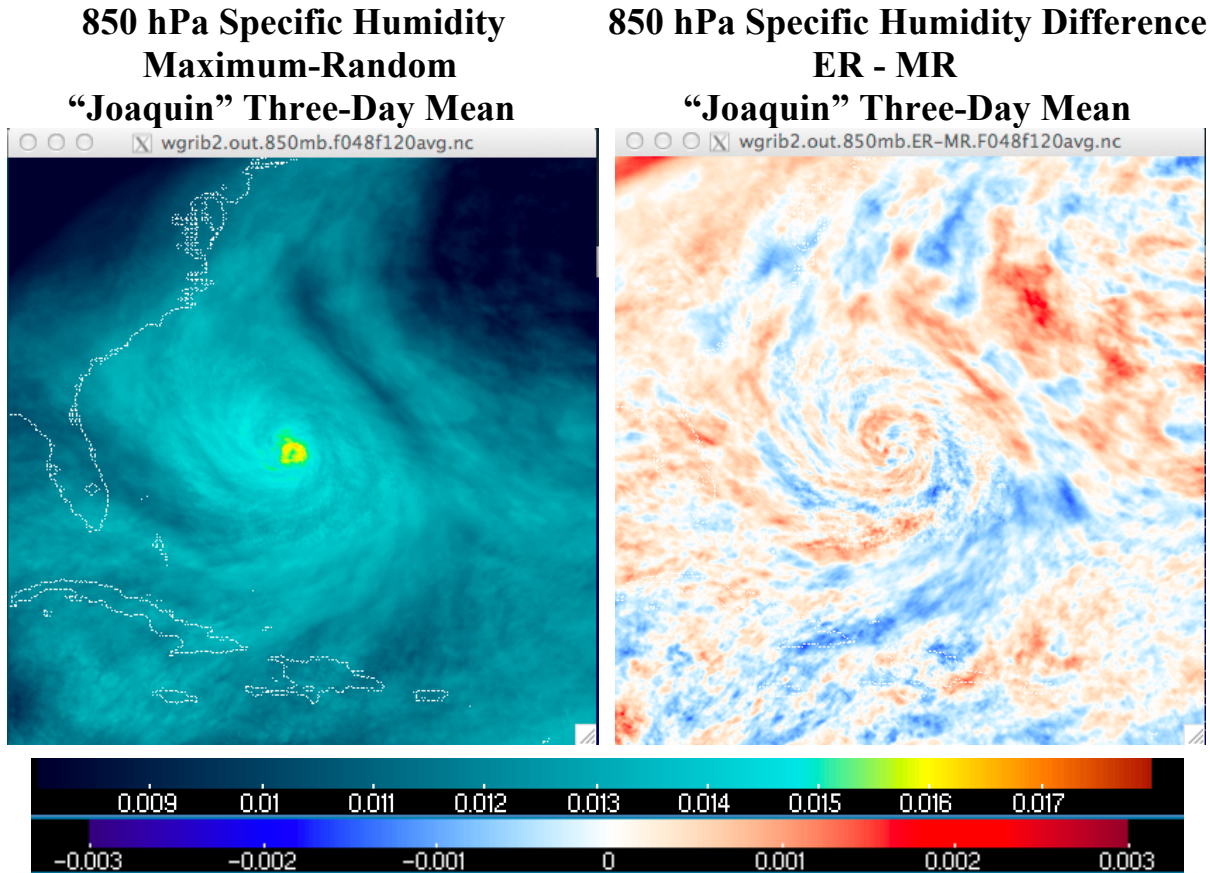


**Figure 15.** Three-day mean 850 hPa specific humidity in the vicinity of Hurricane Joaquin as predicted by HWRP using MR cloud overlap (left) and the three-day mean 850 hPa specific humidity difference for ER-MR cloud overlap (right) averaged over the period from 12 UTC 30 September 2015 to 12 UTC 3 October 2015 from a forecast cycle initialized at 12 UTC 28 September 2015. Plotted data are from the storm-following 6-km nested grid. Red colors in the right panel signify more moisture in the forecast with ER cloud overlap. The geographic range of the plotted area moved over the three-day period, but it is roughly 16N to 41N and 84W to 59W. Units are  $\text{kg kg}^{-1}$ .

The temperature field changes in Figure 14 suggest resulting circulation impacts that may affect the advection of water vapor. The left panel of Figure 15 shows the 850 hPa specific humidity averaged over the same three-day interval from the same HWRP forecast shown in Figure 14. Values as high as  $16 \text{ g kg}^{-1}$  are present within the eye wall of Hurricane Joaquin at the center of the image. The right panel in Figure 15 shows the corresponding three-day mean 850 hPa specific humidity difference (ER-MR) between the two forecasts using each cloud overlap method. Specific humidity differences are highly variable, though with some apparent relation to the spiral banding of the TC. The largest differences appear to be associated with the dry air to the northeast of the hurricane, which may relate to the strength or position of high pressure in that quadrant.

Of greater direct relevance to TC track than temperature and moisture are the upper level winds in the vicinity of the storm that can influence its direction. The left panel of Figure 16 shows the 200 hPa wind speed averaged over the same three-day period and for the same forecasts in Figure 14. Strong winds of 35 to 45 m/s from the south (directions not shown) during this time are apparent over the southeastern U.S. in the upper left corner of the image.

Meanwhile, very weak steering currents are present over the hurricane at the center of the left panel in Figure 16, resulting in its slow movement over this period in some of these forecasts. The wind speed difference between the two overlap methods (ER-MR) averaged over the same three days is shown in the right panel of Figure 16. The most significant result shown is the substantially (roughly 20%) slower wind speeds within the area of strong southerly winds (directions not shown) over the southeastern U.S. in the HWRF forecast using the ER cloud overlap. Stronger 200 hPa winds are seen to the northeast and southeast of the storm center with ER overlap. Figure 16 demonstrates the strong potential for the change from MR to ER cloud overlap to impact the wind fields that can influence modeled storm tracks.

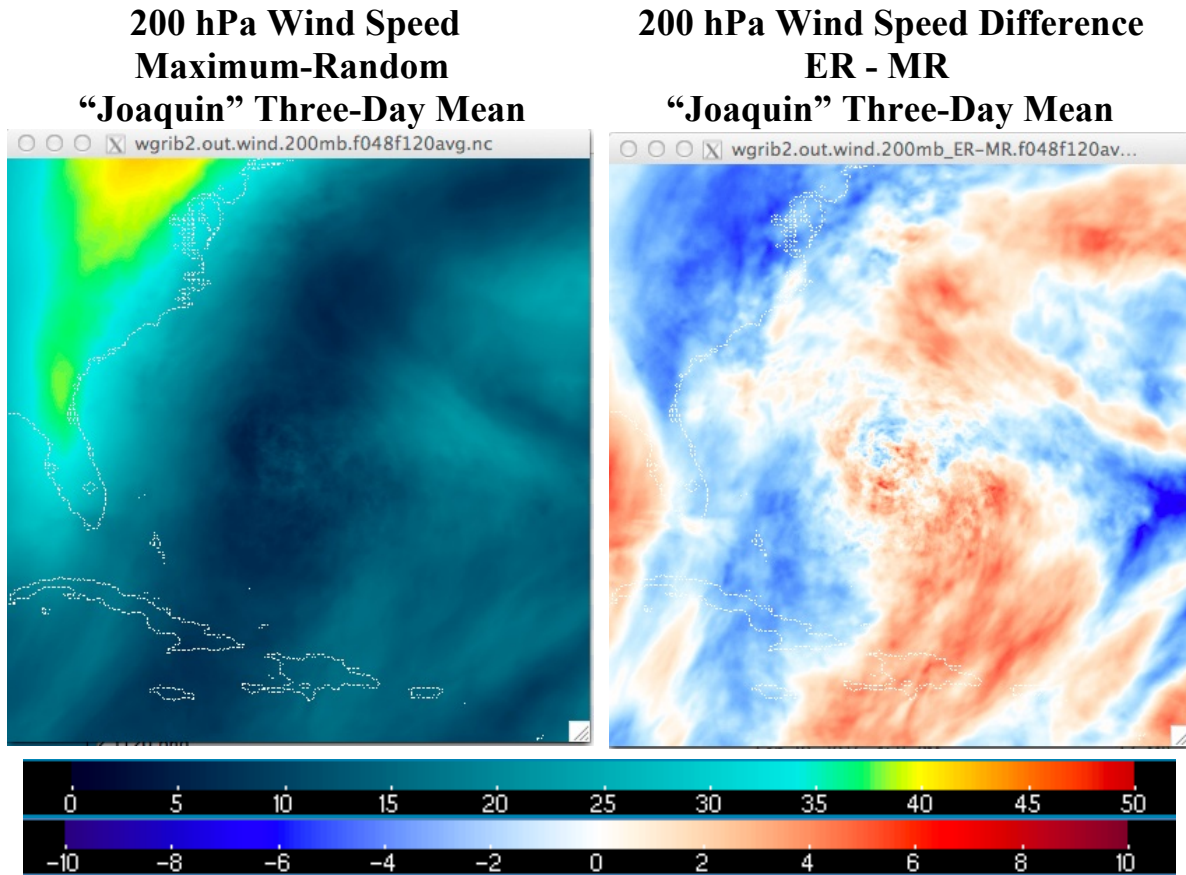


**Figure 16.** Three-day mean 200 hPa wind speed in the vicinity of Hurricane Joaquin as predicted by HWRF using MR cloud overlap (left) and the three-day mean 200 hPa wind speed difference for ER-MR cloud overlap (right) averaged over the period from 12 UTC 30 September 2015 to 12 UTC 3 October 2015 from a forecast cycle initialized at 12 UTC 28 September 2015. Plotted data are from the storm-following 6-km nested grid. Red colors in the right panel signify stronger winds in the forecast with ER cloud overlap. The geographic range of the plotted area moved over the three-day period, but it is roughly 16N to 41N and 84W to 59W. Units are m/s.

### *TC Track and Intensity Impacts*

An important objective of any enhancement to tropical cyclone predictions is the noticeable improvement in the skill of forecasting TC track and intensity. The previous sections have shown that changing from MR to ER cloud overlap has significant impacts on radiative fluxes and heating rates and on atmospheric fields, and this section will illustrate the degree to which these changes effect the track and intensity of the TCs examined in this study. As plotted

by the GFDL vortex tracking software from HWRP model output, Figure 17 shows the track of Hurricane Joaquin for five-day forecast cycles initialized at 00 UTC on 28 September 2015 (left panel) and at 12 UTC on 28 September 2015 (right panel) as predicted by HWRP using the H215 version of the model (green), the H216 version using MR overlap (blue) and the H216 version using ER cloud overlap (red). The best track analysis position of the center of Hurricane Joaquin is shown in white in Figure 17. It should be noted that the H215 model used RRTMG with MR overlap and the H216 model included other physics changes relative to the H215 model. For the forecast cycle initialized at 00 UTC on 28 September 2015, the H215 and H216/MR models bring the TC westward from its initial position over several days, then they bring it directly up the East Coast, while the H216/ER forecast matches the initial westward motion while keeping the storm center relatively stationary for the rest of the forecast. All three forecasts are significantly different from the best-track position of the TC over this time period. For the forecast cycle initialized at 12 UTC on 28 September 2015, the H215 model still brings the TC up the East Coast while the two H216 forecasts both keep the storm further south before turning the TC to the northeast, though ultimately in slightly different positions that are both further north than the best-track analysis.

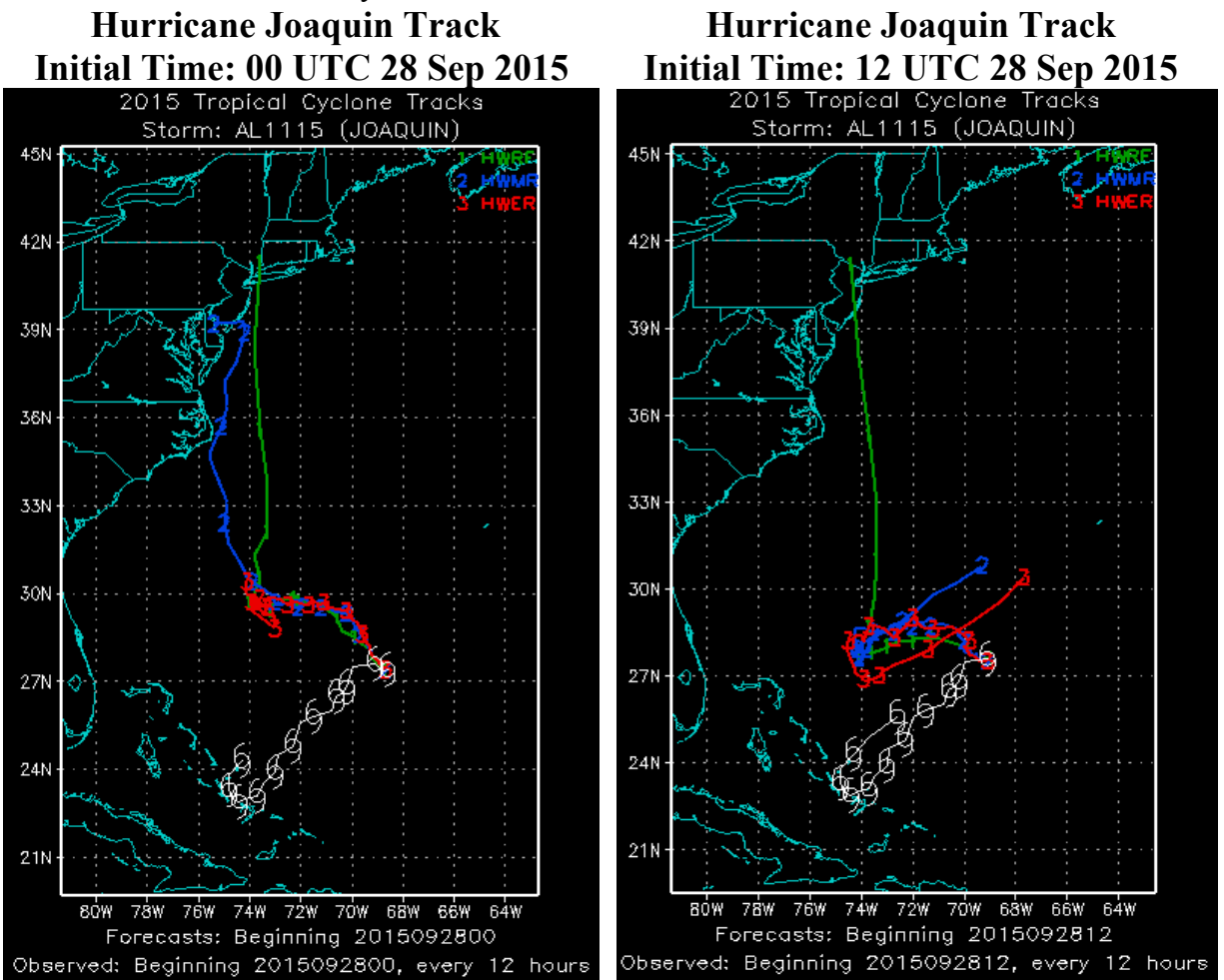
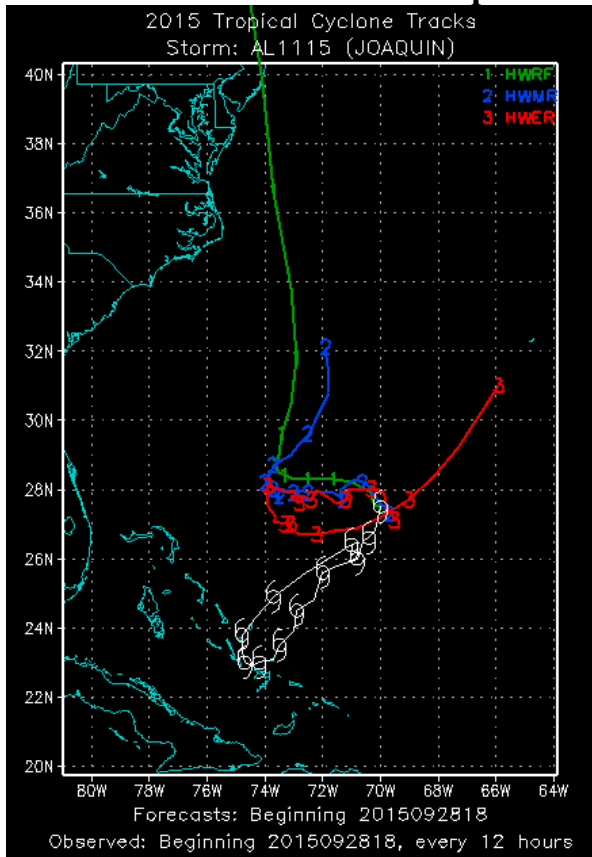


**Figure 17.** Hurricane Joaquin track over five-day forecast cycles starting at 00 UTC 28 September 2015 (left) and at 12 UTC on 28 September 2015 (right) as predicted using three versions of HWRP including the H215 version of the model (green), the H216 version using MR overlap (blue) and the H216 version using ER cloud overlap (red). Also shown is the best track analyzed position of Hurricane Joaquin over the same time period (white).

### Hurricane Joaquin Track Initial Time: 18 UTC 28 Sep 2015



### Hurricane Joaquin Track Initial Time: 00 UTC 29 Sep 2015

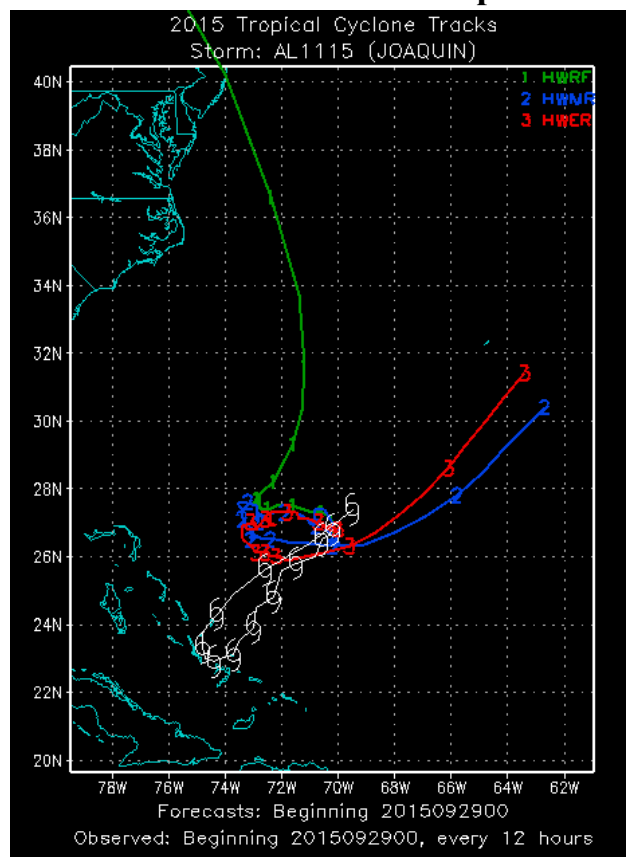
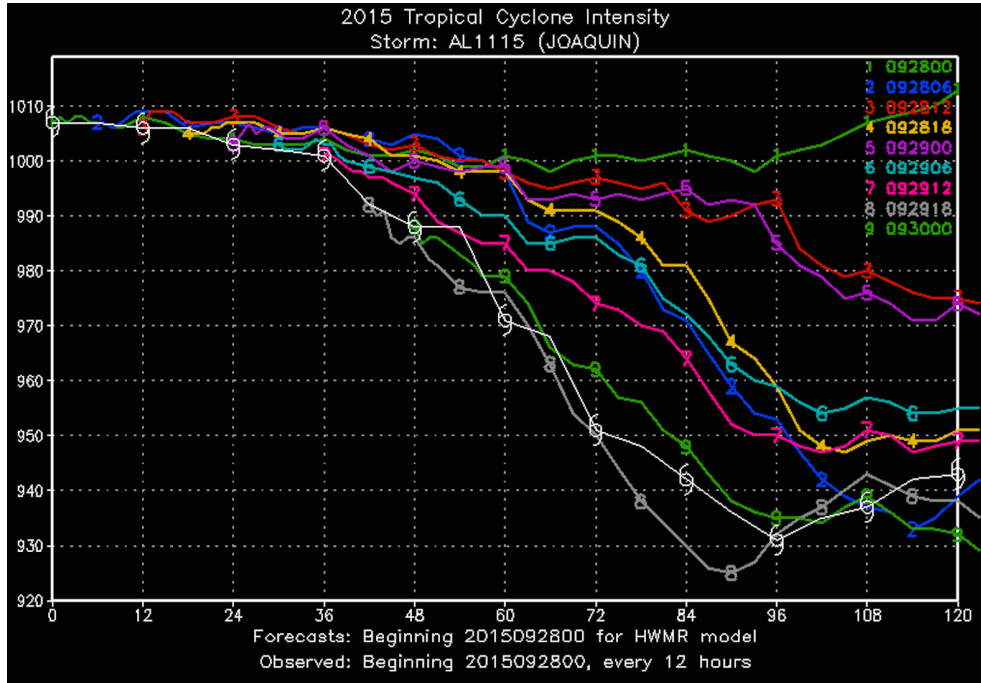


**Figure 18.** Hurricane Joaquin track over five-day forecast cycles starting at 18 UTC 28 September 2015 (left) and at 00 UTC on 29 September 2015 (right) as predicted using three versions of HWRP including the H215 version of the model (green), the H216 version using MR overlap (blue) and the H216 version using ER overlap (red). Also shown is the best track analyzed position of Hurricane Joaquin over the same time period (white).

Hurricane Joaquin tracks predicted with the same versions of HWRP identified in Figure 17 for two subsequent forecast cycles initialized at 18 UTC 28 September 2015 and 00 UTC 29 September 2015 are shown in Figure 18. In the former forecast cycle (left panel), there are substantial differences among the three forecasts shown, while in the latter cycle (right panel) both of the H216 forecasts diverge significantly from the H215 forecast while tracking relatively close to each other. Both of the H216 forecasts are similar in the right panel of Figure 18, though each turns the TC toward the northeast at a point much further north than the analyzed track. Differences to varying degrees are noted between the H216/MR and H216/ER track forecasts in all four forecast cycles shown, suggesting a complex relationship between the impacts of the cloud overlap change on the atmospheric state and their role in affecting the predicted track for Hurricane Joaquin.

Tropical cyclone intensity is typically diagnosed through its central surface pressure and maximum surface wind speed. Time series of the 6-hourly central surface pressure for Hurricane Joaquin as predicted by HWRP using MR (top panel) and ER (bottom panel) cloud overlap over

## Hurricane Joaquin Intensity (Central Pressure) H216 Maximum-Random



## Hurricane Joaquin Intensity (Central Pressure) H216 Exponential-Random

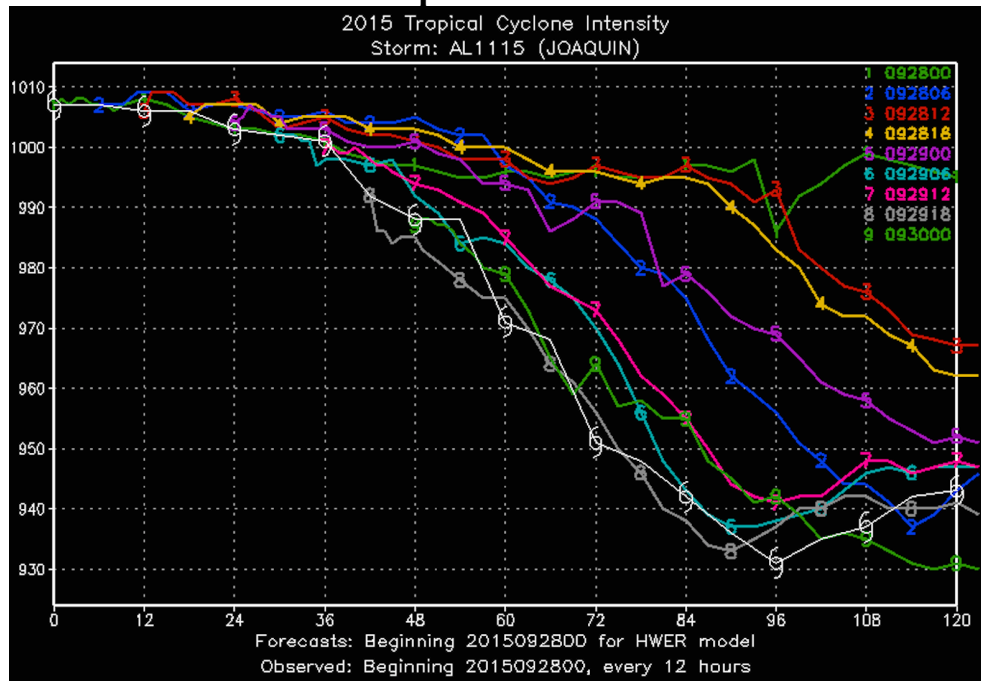
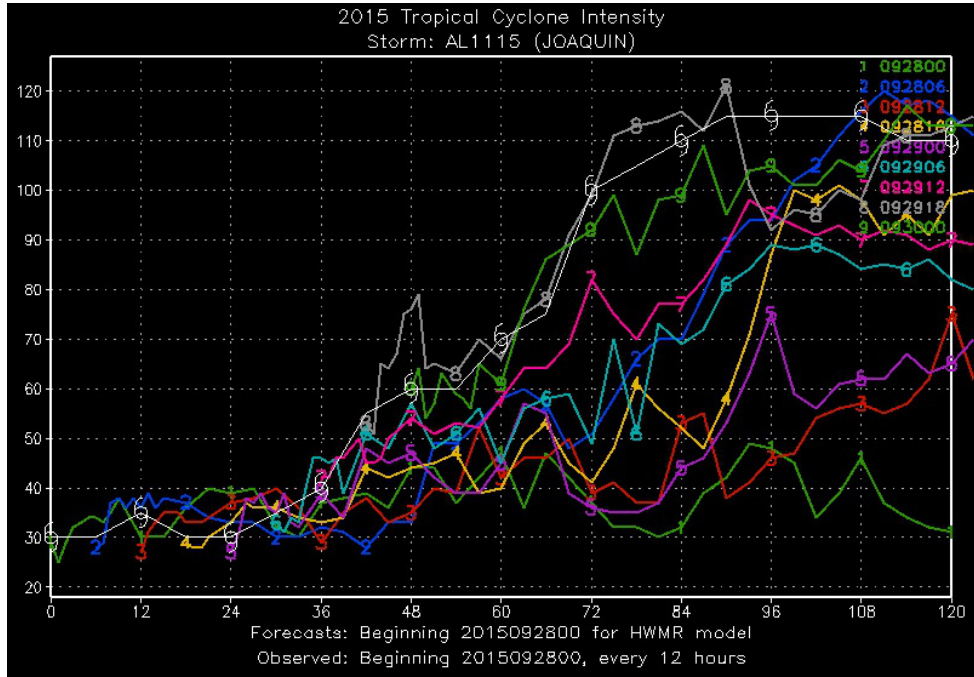


**Figure 19.** Hurricane Joaquin central pressure intensity over nine five-day forecast cycles initialized at six hour intervals from 00 UTC on 28 September 2015 through 00 UTC on 30 September 2015 as predicted by the H216 model using the maximum-random cloud overlap method (top panel) and using the exponential-random cloud overlap method (bottom panel). The x-axis unit is hours and the y-axis unit is hPa.

## Hurricane Joaquin Intensity (Maximum Wind Speed) H216 Maximum-Random



## Hurricane Joaquin Intensity (Maximum Wind Speed) H216 Exponential-Random

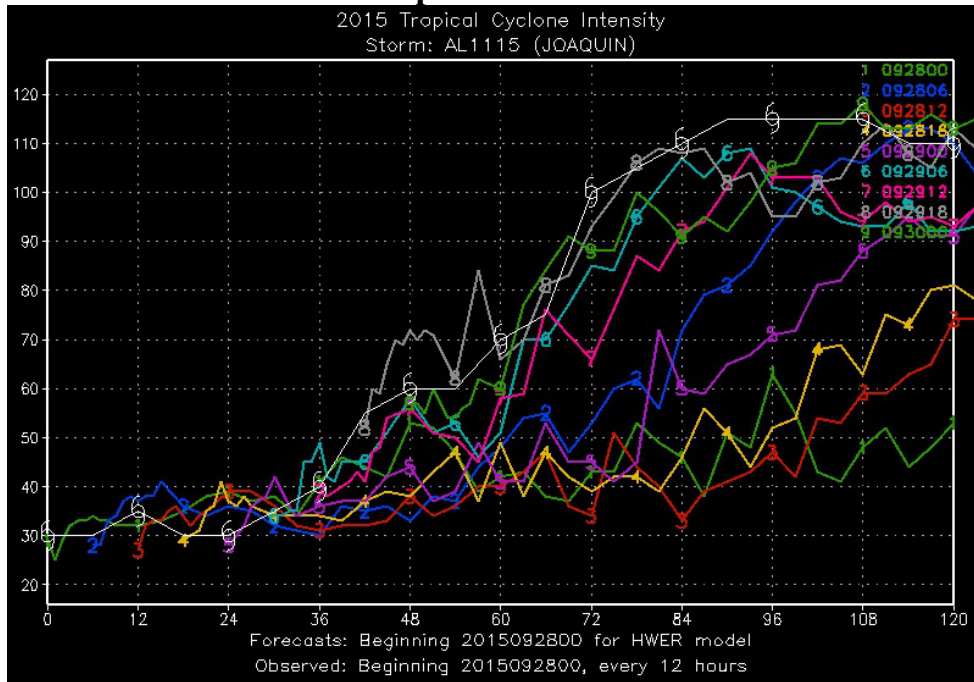


**Figure 20.** Hurricane Joaquin maximum wind speed intensity over nine five-day forecast cycles initialized at six hour intervals from 00 UTC on 28 September 2015 through 00 UTC on 30 September 2015 as predicted by the H216 model using the maximum-random cloud overlap method (top panel) and using the exponential-random cloud overlap method (bottom panel). The x-axis unit is hours and the y-axis unit is knots.

nine continuous forecast cycles initialized at six hour intervals from 00 UTC 28 September 2015 to 00 UTC 30 September 2015 is shown in Figure 19. The analyzed minimum surface pressure at each time is also shown in white. Judging by this measure, the forecasts with ER overlap produced surface pressures closer to the analysis for several forecast cycles (for example, those plotted in purple, magenta and cyan in Figure 19), while one forecast cycle was noticeably better with MR overlap (plotted in yellow). It is notable that in addition to forecasting Joaquin too far north relative to the actual storm (Figures 17 and 18), HWRf produces a storm that is generally too weak over these forecast cycles as well. Of course, hurricane track and intensity forecasts are closely related in that TC intensity is likely influenced by its location within the surrounding environment and the intensity may be influenced by track errors. Similar plots showing the maximum surface wind speed from each forecast for the same set of forecast cycles is shown in Figure 20, and the analyzed maximum wind speed is plotted in white. The relative impact of the cloud overlap change on wind speed is consistent with the surface pressure forecasts.

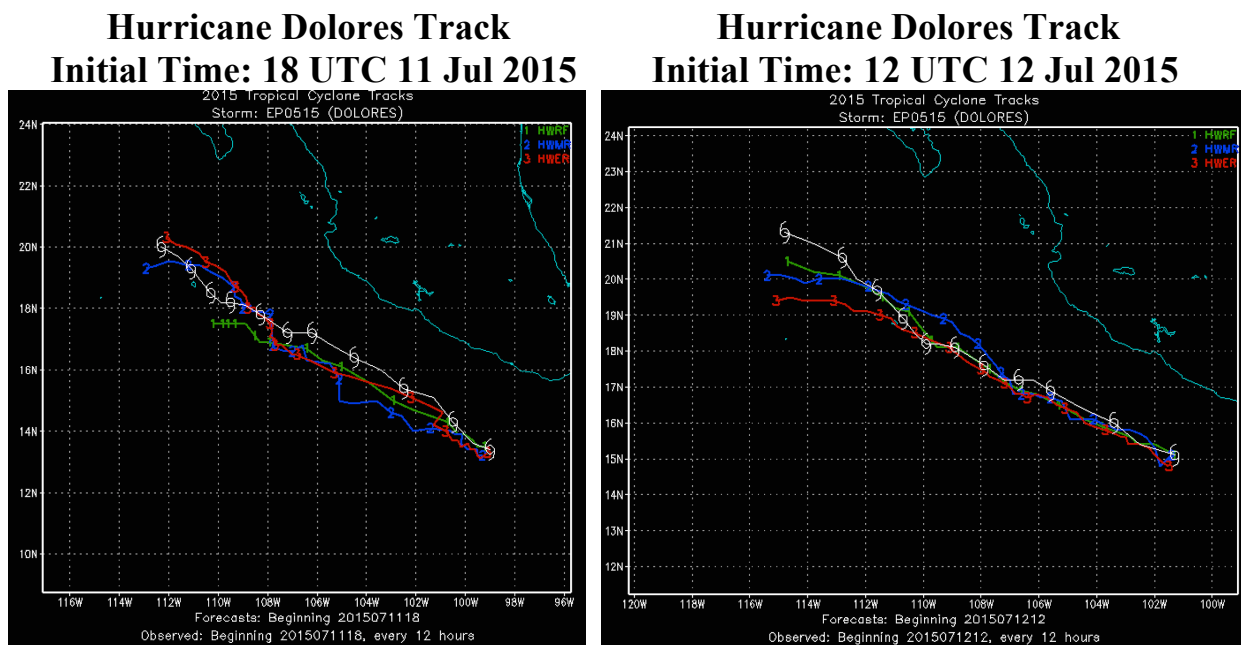
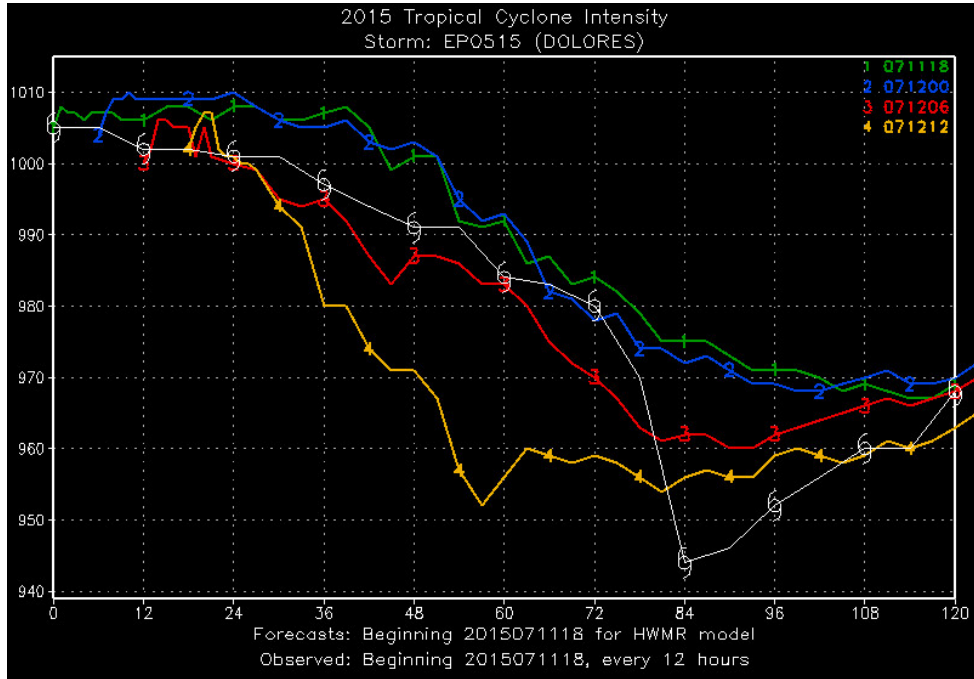


**Figure 21.** Hurricane Dolores track over five-day forecast cycles starting at 18 UTC 11 July 2015 (left) and at 12 UTC on 12 July 2015 (right) as predicted using three versions of HWRf including the H215 version of the model (green), the H216 version using MR overlap (blue) and the H216 version using ER overlap (red). Also shown is the best track analyzed position of Hurricane Dolores over the same time period (white).

The cloud overlap change has less of an impact on the evolution of Hurricane Dolores and its track northwestward through the East Pacific than it does on Hurricane Joaquin, as illustrated in Figure 21. This figure shows the predicted track of Dolores as predicted by the H215 model (green), the H216 model using MR overlap (blue) and the H216 model using ER overlap (red) for two forecast cycles initialized at 18 UTC 11 July 2015 (left panel) and at 12 UTC 12 July 2015 (right panel). Although there are small deviations between each model configuration and the best track position each forecast generally follows a similar path parallel to the coast of Central America. One exception is the final day of the forecast cycle initialized at 12 UTC on 12 July 2015, during which the predicted tracks diverge from the analyzed positions, possibly in response to changes in the synoptic scale features at higher latitudes.

## Hurricane Dolores Intensity (Central Pressure) H216 Maximum-Random



## Hurricane Dolores Intensity (Central Pressure) H216 Exponential-Random

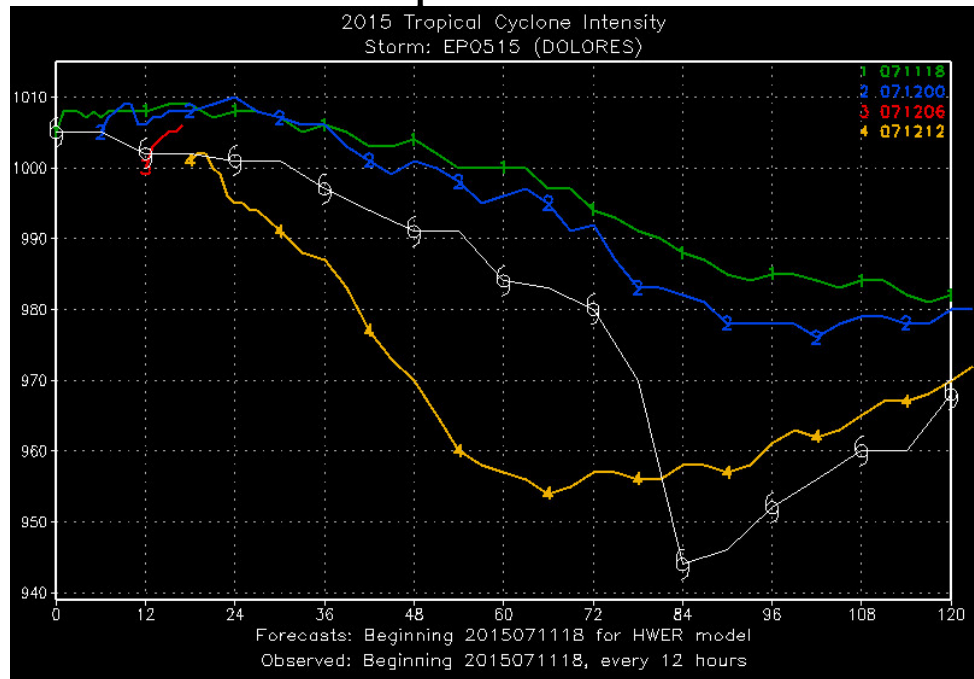
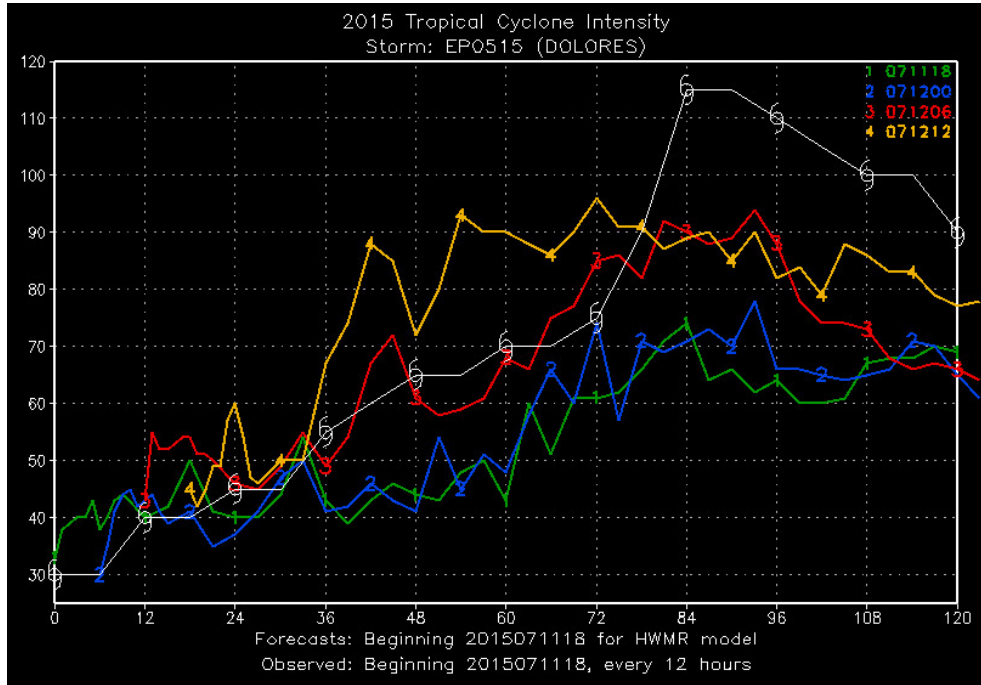


**Figure 22.** Hurricane Dolores central pressure intensity over five-day forecast cycles initialized at six hour intervals from 18 UTC on 11 July 2015 through 12 UTC on 12 July 2015 as predicted by the H216 model using the maximum-random cloud overlap method (top panel) and using the exponential-random cloud overlap method (bottom panel). The x-axis unit is hours and the y-axis unit is hPa.

## Hurricane Dolores Intensity (Maximum Wind Speed) H216 Maximum-Random



## Hurricane Dolores Intensity (Maximum Wind Speed) H216 Exponential-Random

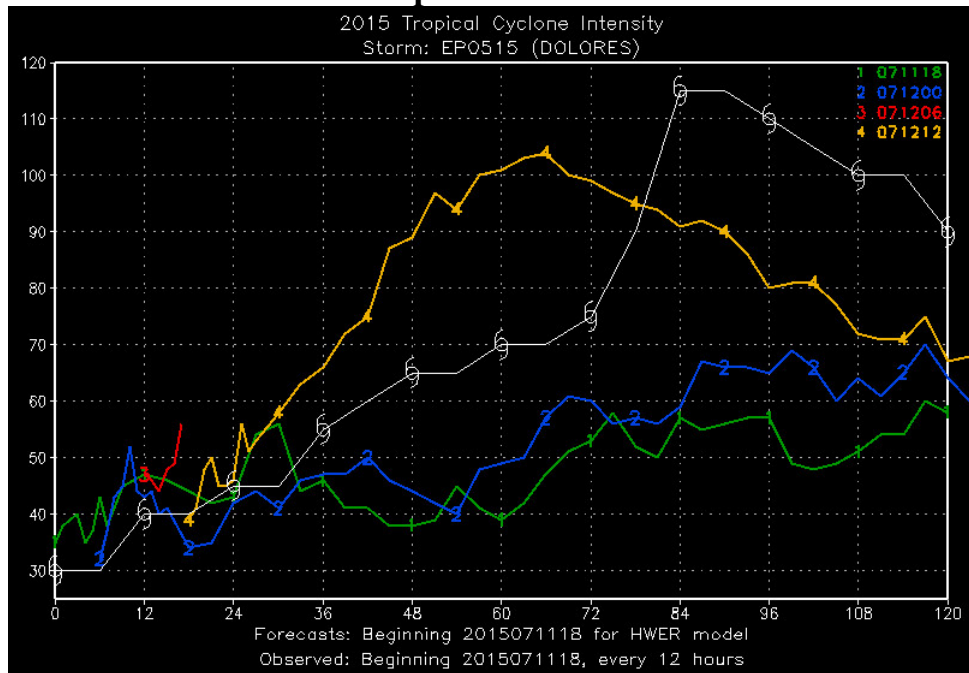


**Figure 23.** Hurricane Dolores maximum wind speed intensity over five-day forecast cycles initialized at six hour intervals from 18 UTC on 11 July 2015 through 12 UTC on 12 July 2015 as predicted by the H216 model using the maximum-random cloud overlap method (top panel) and using the exponential-random cloud overlap method (bottom panel). The x-axis unit is hours and the y-axis unit is knots.

Changes in Hurricane Dolores central pressure intensity caused by the cloud overlap modification are shown for several forecast cycles in Figure 22. The ER overlap (bottom panel) appears to produce a weaker vortex in the two earliest forecast cycles (green and blue) relative to the forecast using MR overlap (top panel). The central pressure is very similar between the two runs for a later forecast cycle (yellow), which is initially too strong, but captures the analyzed weakening trend during the fourth and fifth days. These observations are similar for the modeled and best track maximum wind speeds for the same forecast cycles shown in Figure 23. Though none of the predicted wind speeds reach the highest analyzed wind speed in this period of 115 knots, the forecasts with MR overlap for the first two forecast cycles shown (green and blue) are slightly stronger than the TC generated using ER overlap. In contrast, the ER forecast produces a stronger hurricane (with maximum winds over 100 knots) than the MR forecast, although this intensity is reached earlier than the analyzed maximum wind speeds.

As with Dolores, predictions of Hurricane Gonzalo show only small variations between the H215 model and the H216 model using each cloud overlap method as shown in Figure 24 for the two forecast cycles tested for this TC. Throughout the forecast cycle initialized at 00 UTC 13 October 2014 (left panel), the model tracks are nearly identical, while in the forecast cycle initialized six hours later (right panel), the predicted tracks deviate from the best track positions by 50-100 km toward the end of the five-day period, though the pair of H216 forecasts remain close to each other.

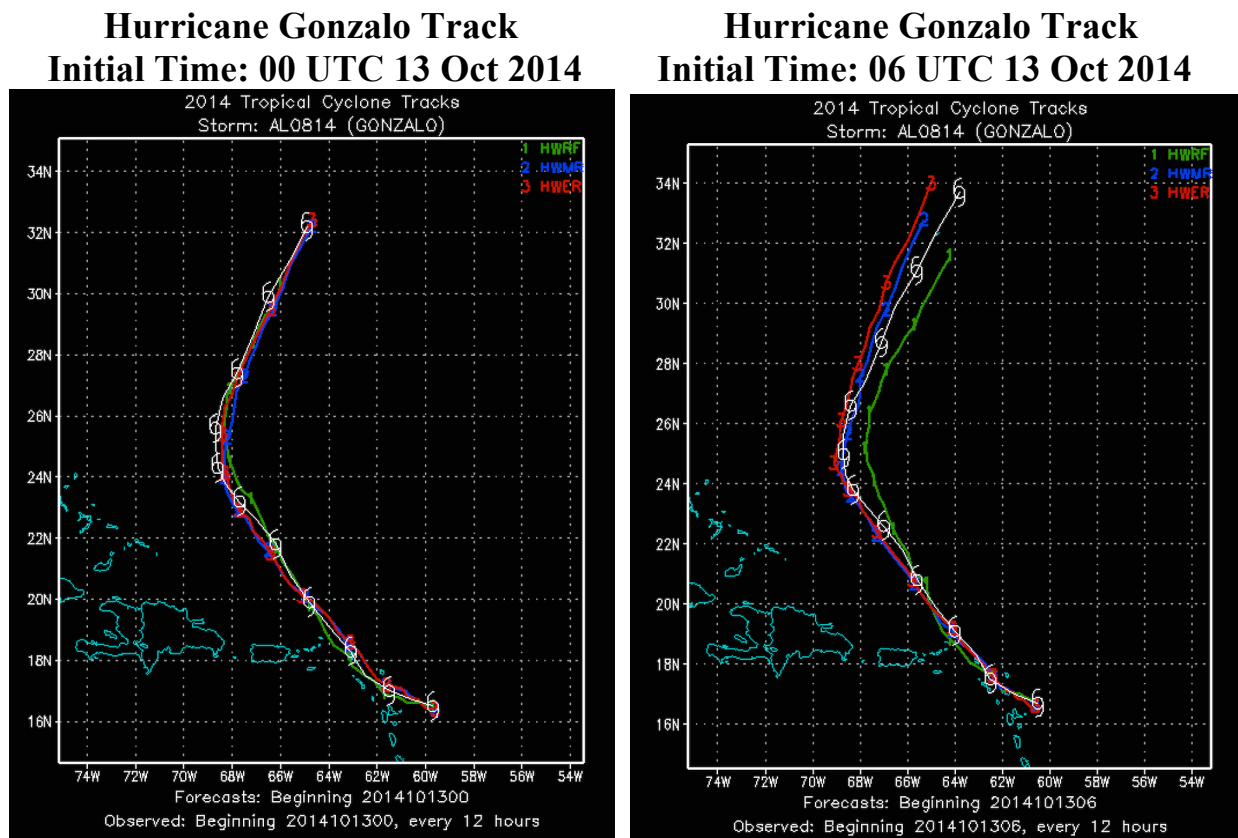
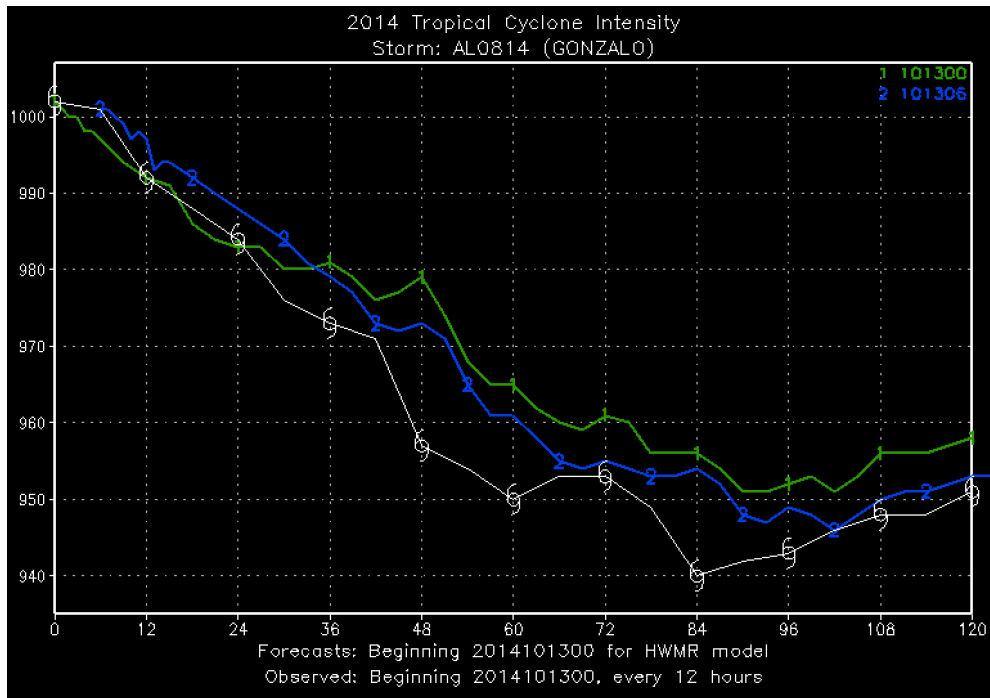


**Figure 24.** Hurricane Gonzalo track over five-day forecast cycles starting at 00 UTC 13 October 2014 (left) and at 06 UTC on 13 October 2014 (right) as predicted using three versions of HWRP including the H215 version of the model (green), the H216 version using MR overlap (blue) and the H216 version using ER overlap (red). Also shown is the best track analyzed position of Hurricane Gonzalo over the same time period (white).

## Hurricane Gonzalo Intensity (Central Pressure) H216 Maximum-Random



## Hurricane Gonzalo Intensity (Central Pressure) H216 Exponential-Random

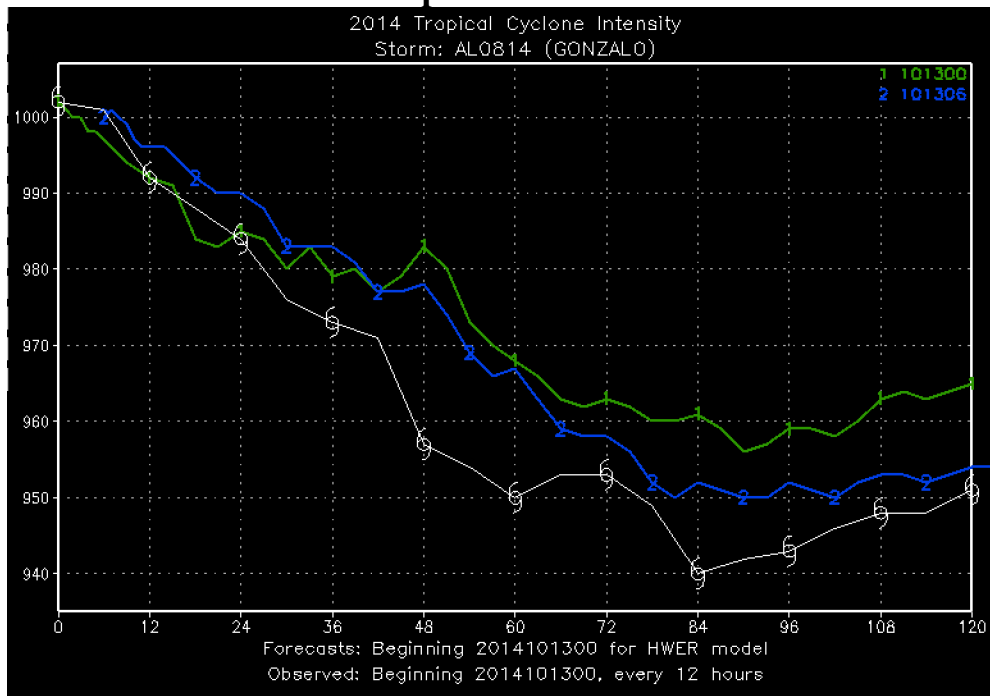
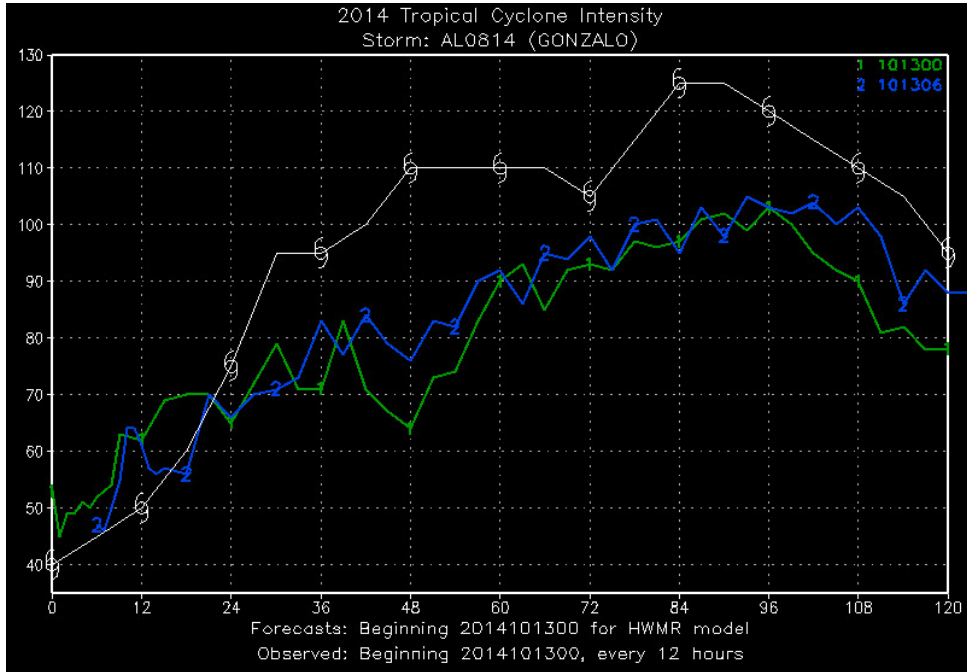


**Figure 25.** Hurricane Gonzalo central pressure intensity over two five-day forecast cycles initialized at 00 UTC on 13 October 2014 and 06 UTC on 13 October 2014 as predicted by the H216 model using the maximum-random cloud overlap method (top panel) and using the exponential-random cloud overlap method (bottom panel). The x-axis unit is hours and the y-axis unit is hPa.

## Hurricane Gonzalo Intensity (Maximum Wind Speed) H216 Maximum-Random



## Hurricane Gonzalo Intensity (Maximum Wind Speed) H216 Exponential-Random

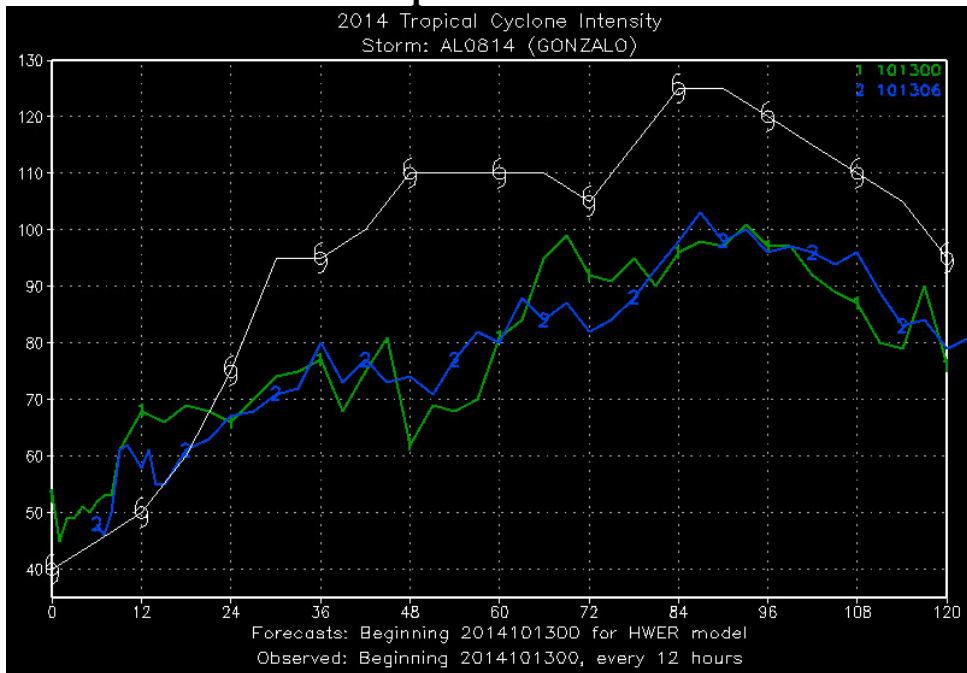


**Figure 26.** Hurricane Gonzalo maximum wind speed intensity over five-day forecast cycles initialized at six hour intervals from 00 UTC on 13 October 2014 through 06 UTC on 13 October 2014 as predicted by the H216 model using the maximum-random cloud overlap method (top panel) and using the exponential-random cloud overlap method (bottom panel). The x-axis unit is hours and the y-axis unit is knots.

Little impact was noted on the intensity of Hurricane Gonzalo due to the cloud overlap change as shown in Figure 25 for central pressure and in Figure 26 for maximum wind speeds for the two forecast cycles shown in Figure 24. In each case, the predicted intensity remains too weak relative to the best track analyzed values over these time periods, though the modeled hurricanes reach their maximum intensity close to the observed time.

#### **4. Conclusions and Future Work**

The goal of this project was to illustrate the potential for modifications to the cloud overlap assumption applied in the radiation code to influence the radiative fluxes and heating rates, the atmospheric state, and ultimately the track and intensity of tropical cyclones predicted by HWRF. The cloud overlap change tested involved replacing the commonly used maximum-random method with an exponential-random approach that relaxes the strict assumption of maximum overlap through adjacent cloud layers by allowing the vertical correlation of clouds to transition exponentially from maximum to random with distance through the cloud. A constant decorrelation length scale of 2 km was used in the TC forecasts completed for this project, though the selection of the optimal decorrelation length to use at a given latitude or for a specific cloud configuration requires further research. The physics change was tested using the H216 model (with the ICLLOUD=3 name-list option for defining fractional cloudiness) and the RRTMG longwave and shortwave radiation codes. Forecasts using each cloud overlap method were completed for multiple forecast cycles of Hurricanes Joaquin, Dolores and Gonzalo.

Several primary conclusions can be drawn from the work completed during this project. First, it was shown that predicted radiative heating rate profiles reflect the influence of all of the atmospheric state variables ingested into the radiation code and provide detailed information related to the inner structure of tropical cyclones, though heating rate verification options remain limited. Second, the single change of relaxing the strict maximum overlap assumption through adjacent cloud layers to allow an exponential decay of the vertical cloud correlation from maximum to random with greater distance through the adjacent clouds has been shown to significantly alter the radiative heating rates and fluxes in the predicted tropical cyclones. Third, these radiative changes in turn also modify the atmospheric state both within the TC and in the surrounding environment over time, and in at least several forecast cycles of one case studied (Hurricane Joaquin) large changes in TC track and intensity resulted.

Given the magnitude of the changes to the atmospheric environment and TC track and intensity seen in one of the three cases studied for this project, the implications of effectively treating the radiative influence of the vertical correlation of fractional clouds (as well as the parameterization of fractional cloudiness itself) requires further investigation. Work is ongoing within the DTC to evaluate the cloud overlap change for a larger number of TC cases to provide a better statistical basis for assessing its impact. In addition, a name-list option to switch between the MR and ER cloud overlap options (and possibly the decorrelation length value) will be installed to support testing of this option at the request of NOAA/EMC. Finally, additional cloud overlap related modifications that will be tested in the future include applying different constant values for the decorrelation length and developing a decorrelation length that varies spatially either by latitude or in response to specific atmospheric parameters such as water vapor, cloud properties, or variations in wind speed with height.

## 5. Project Deliverables

This project generated several deliverables for the DTC including the exponential-random cloud overlap source code added to RRTMG, two presentations (one for NCAR and one for NOAA) and the final project report (this document).

Iacono, M.J., and J.M. Henderson, Testing revisions to RRTMG cloud radiative transfer in HWRF, Project Final Report, Developmental Testbed Center, March 2017.

Iacono, M.J., and J.M. Henderson, The impact of changing the RRTMG cloud overlap method on tropical cyclone evolution in HWRF, Seminar presented to the National Oceanic and Atmospheric Administration Environmental Modeling Center Hurricane Team Weekly Seminar Series, November 9, 2016.

Iacono, M.J., and J.M. Henderson, The impact of changing the RRTMG cloud overlap method on tropical cyclone evolution in HWRF, Seminar presented for the Developmental Testbed Center Visitor Program, National Center for Atmospheric Research, Foothills Laboratory, Boulder, Colorado, October 14, 2016.

## 6. References

Barker, H., J.N.S. Cole, J.-J. Morcrette, R. Pincus, P. Raisanen, Monte Carlo Independent Column Approximation (McICA): Up and running in North America and Europe, Talk presented at the 17th Atmospheric Radiation Measurement (ARM) Science Team Meeting, Monterey, CA, March 26-30, 2007.

Bernardet, L., V. Tallapragada, S. Bao, S. Trahan, Y. Kwon, Q. Liu, M. Tong, M. Biswas, T. Brown, D. Stark, L. Carson, R. Yablonsky, E. Uhlhorn, S. Gopalakrishnan, X. Zhang, T. Marchok, B. Kuo, and R. Gall, Community Support and Transition of Research to Operations for the Hurricane Weather Research and Forecasting Model. *Bull. Amer. Meteor. Soc.*, 96, 953–960, 2015.

Geer, A.J., P. Bauer, and C.W. O'Dell, A revised cloud overlap scheme for fast microwave radiative transfer in rain and cloud, *J. Climate*, 48, 2257–2270, 2009.

Geleyn, J.F., Hollingsworth, A., An economical, analytical method for the computation of the interaction between scattering and line absorption of radiation, *Contrib. Atmos. Phys.*, 52, 1–16, 1979.

Hogan, R.J., Illingworth, A.J., Deriving cloud overlap statistics from radar. *Q. J. R. Meteorol. Soc.*, 126, 2903–2909, 2000.

Iacono, M.J., J.S. Delamere, E.J. Mlawer, M.W. Shephard, S.A. Clough, and W.D. Collins, Radiative forcing by long-lived greenhouse gases: calculations with the AER radiative transfer models, *J. Geophys. Res.*, 113, D13103, doi:10.1029/2008JD009944, 2008.

Mace, G.G., and S. Benson-Troth, Cloud-layer overlap characteristics derived from long-term cloud radar data, *J. Climate*, 15, 2505–2515, 2002.

Nam, C., S. Bony, J.-L. Dufresne, and H. Chepfer, The ‘too few, too bright’ tropical low-cloud problem in CMIP5 models, *Geophys. Res. Lett.*, 39, L21801, doi:10.1029/2012GL053421, 2012.

Naud, C., A. Del Genio, G.G. Mace, S. Benson, E.E. Clothiaux, P. Kollias, Impact of dynamics and atmospheric state on cloud vertical overlap, *J. Climate*, 21, 1758–1770, 2008.

Pincus, R., C. Hannay, S. A. Klein, K.-M. Xu, and R. Hemler, Overlap assumptions for assumed

- probability distribution function cloud schemes in large-scale models, *J. Geophys. Res.*, 110, D15S09, doi:10.1029/2004JD005100, 2005.
- Pincus, R., H. W. Barker, J.-J. Morcrette, A fast, flexible, approximate technique for computing radiative transfer in inhomogeneous cloud fields, *J. Geophys. Res.*, 108, D13, 2003.
- Shonk, J.K.P., R.J. Hogan, J.M. Edwards, and G.G. Mace, Effect of improving representation of horizontal and vertical cloud structure on the Earth's global radiation budget. Part I: Review and parametrization, *Q. J. R. Meteorol. Soc.*, 136, 1191–1204, 2010a.
- Shonk, J.K.P., and R.J. Hogan, Effect of improving representation of horizontal and vertical cloud structure on the Earth's global radiation budget. Part II: The global effects, *Q. J. R. Meteorol. Soc.*, 136, 1205–1215, 2010b.
- Tourville, N., G. Stephens, M. DeMaria, and D. Vane, Remote Sensing of Tropical Cyclones: Observations from CloudSat and A-Train Profilers. *Bull. Amer. Meteor. Soc.*, **96**, 609–622, 2015.
- Wu, X., and X.-Z. Liang, Radiative effects of cloud horizontal inhomogeneity and vertical overlap identified from a month-long cloud resolving simulation, *J. Atmos. Sci.*, 62, 4105–4112, 2005.